

BACHELOR THESIS

Hybrid Aircraft - State-of-the-art of main components and simulation
of its power grid

WRITTEN BY

Moritz Kraus

Examiner: Prof. Dr. Sergio Montenegro, Julius-Maximilians-University Würzburg, Germany

3rd August 2020

Abstract

Electric and hybrid aircraft propulsion systems are highly researched topics in both the aviation industry and at research institutions. In this thesis the state-of-the-art of hybrid propulsion system components (electric motors, batteries and gas turbines) and the technical background of hybrid propulsion system are presented. Advantages and disadvantages of different hybrid architectures are demonstrated and potentials of hybrid propulsion systems are explained. The biggest issue of hybrid propulsion systems, the limited energy density of modern batteries, will be covered as well. Typical consumers of electrical energy in aircraft are displayed. In addition promising plane concepts (mostly electric) are presented.

In the second part, a simulation tool will be presented which simulates the energy levels of chemical and electrical energy storages during the flight of a hybrid aircraft, and the results of one simulation are displayed. The tool produces plots of energy levels, mass loss during cruise and required power for instance.

Metrics to evaluate the performance of the simulated aircraft are presented and discussed. These metrics include ranges for the simulated hybrid, electric and conventional aircraft with the same parameters. Total costs and CO₂ emissions are calculated as well as additional aircraft descriptive parameters (Degree of Hybridization, ESAR, TSPC). An adaption of the classical range equation by Breguet is presented.

Declaration of Authorship

I declare that I completed this thesis on my own and that information which has been directly or indirectly taken from other sources has been noted as such. Neither this nor a similar work has been presented to an examination committee.

Name of Student: Moritz Kraus

Würzburg, 3rd August 2020



Moritz Kraus

Contents

1	Introduction	1
1.1	Problem formulation	1
1.2	Outline	2
2	Background	3
2.1	Technical background of hybrid planes	3
2.1.1	Hybrid power trains	3
2.1.1.1	Types	3
2.1.1.2	Advantages	5
2.1.1.3	Disadvantages	5
2.1.1.4	Potentials	6
2.2	Subsystems	6
2.2.1	Electric motors	6
2.2.1.1	Siemens/Rolls-Royce	7
2.2.1.2	Emrax	7
2.2.1.3	MagniX	7
2.2.1.4	Comparison	8
2.2.2	Gas turbines	8
2.2.2.1	Safran	9
2.2.2.2	General Electric	10
2.2.2.3	Rolls-Royce	10
2.2.2.4	Comparison	11
2.2.3	Batteries	11
2.2.3.1	Theory and problems	12
2.2.3.2	KOKAM	12
2.2.3.3	BorgWarner	13
2.2.3.4	Summary	13
2.2.4	Electrical loads	14
2.2.4.1	Motor and actuation	14
2.2.4.2	Lighting services	14
2.2.4.3	Heating services	14
2.2.4.4	Subsystem controllers and avionic systems	15
2.2.4.5	Ancillary systems	15
2.2.4.6	Summary	15

2.3 Concept planes	16
2.3.1 Eviation Alice	16
2.3.2 X57 Maxwell	16
2.3.3 Rolls-Royce ACCEL	17
2.3.4 Ampaire 337	18
2.3.5 Summary	18
3 Simulation	20
3.1 Outlook	20
3.2 Structure	20
3.2.1 Running the simulation	21
3.2.2 Simulation.m file	21
3.2.3 writeInput.m file	21
3.2.4 updateGUI.m file	22
3.2.5 computeMetrics.m and computeMeasures.m files	22
3.3 Simulation details	22
3.3.1 Input matrices	22
3.3.1.1 Matrix format	22
3.3.2 Energy storage/propulsion systems modelling	24
3.3.3 Basic simulation	25
3.4 Window frames and theoretical background of shown parameters	26
3.4.1 "Main GUI" window	26
3.4.2 "Input Variables" window	28
3.4.3 "Insights" window	29
3.4.3.1 Operating costs	29
3.4.3.2 CO₂ emissions	30
3.4.3.3 Degree of hybridization	30
3.4.3.4 Combined energy density	31
3.4.4 "Metrics" window	31
3.4.4.1 Required power and weight in cruise	32
3.4.4.2 TSPC (Thrust Specific Power Consumption)	35
3.4.4.3 ESAR (Energy Specific Air Range)	36
3.4.4.4 Ranges	36
3.5 Validation and simulation results	37
3.5.1 Validation data	38
3.5.1.1 Mass breakdown	38
3.5.1.2 Propulsion systems parameters	38
3.5.1.3 Costs and emissions	39
3.5.1.4 Aerodynamic parameters	39
3.5.1.5 Flight matrices	40
3.5.2 Simulation results	40
3.5.2.1 Main simulation	41
3.5.2.2 Costs and emissions	41
3.5.2.3 Degree of hybridization and combined energy density	41
3.5.2.4 Required power and mass loss	42
3.5.2.5 ESAR and TSPC	44

3.5.2.6 Ranges	44
3.5.3 Discussion and analysis	44
4 Conclusion and outlook	46
Bibliography	49

List of Figures

2.1 Serial architecture according to [1], adapted	4
2.2 Parallel architecture according to [1], adapted	4
2.3 Eviation Alice at Paris Airshow 2019; taken from [2]	16
2.4 Computer-simulated figure of X-57 concept; taken from [3]	17
2.5 ACCEL; taken from [4]	18
2.6 Ampaire 337 concept plane; taken from [5]	19
3.1 Architecture of the simulation tool	23
3.2 Screenshot of the "Main GUI window"	27
3.3 Screenshot of "Input Variables" window	28
3.4 Screenshot of "Insights" window	29
3.5 Screenshot of "Metrics" window	32
3.6 Forces in cruise, taken from [6]	33
3.7 Energy levels during flight	41
3.8 Zoom into battery state of charge	42
3.9 Power during cruise	43
3.10 Mass of plane during cruise	43
3.11 ESAR during cruise	44

List of Tables

2.1	Technical specs of different Siemens motors [7][8]	7
2.2	Technical specs of different Emrax motors; due to different submodel types only the general data for each model is given; ratios self calculated; best case values were used for calculation	8
2.3	Technical specs of MagniX motors [9]; ratios self calculated	8
2.4	Technical specs of Arrano [10]	10
2.5	Technical specs of Ardiden family models [11]	10
2.6	Technical specs of MTR390-E [12]	10
2.7	Technical specs of T700 family models	11
2.8	Technical specs of CTS800-4N [13]	11
2.9	Technical specs of AE-2100D2 [14]	11
2.10	Technical data of KOKAM UHE Pack [15]	13
2.11	Technical data of Hermes battery system [16]	13
2.12	Technical specs of X57 Maxwell in final configuration [3]	17
3.1	Mass breakdown of simulated plane based on [17]	38
3.2	Data of the simulated electric propulsion system	38
3.3	Data of the simulated conventional propulsion system	39
3.4	Cost and emission data	39
3.5	Aerodynamic data	40

Chapter 1

Introduction

The modern aviation market is dominated by relatively big aircraft with more than 100 seats, mostly powered by conventional turbofan engines [18]. These engines consume mainly kerosene which emits tons of CO₂ per flight. Global aviation is responsible for around 4% of yearly global emissions of greenhouse gases [19]. As modern society is more aware of the environmental impact of its lifestyle, the aviation industry and other institutions including universities and governmental agencies are trying to make flying more sustainable. Different technologies are being researched, more efficient turbines or synthetic kerosene, which is produced using renewable power. In addition to their impact on sustainability, these technologies can help to reduce costs in the future [20].

The advancements in battery technology and powertrain solutions helped electric cars to rise. Companies like Tesla or Nikola are trying to make electric cars available for the vast majority and lower prices through mass production.

These advancements in battery technology accomplished by these companies and research institutions made all-electric or hybrid planes thinkable. Therefore many electric or hybrid flying research projects and concept planes were launched or will be launched in the near future. Companies like Airbus built prototypes to show the possibilities of electric flying [21], and interesting electric planes like the Eviation Alice will enter market maturity soon [22]. Unfortunately, all-electric planes won't be able to replace conventional planes in near future as battery technology needs to advance even more to achieve energy densities that are comparable to kerosene.

Hybrid flying could be an intermediate stage on the way to an all-electric sustainable aviation industry combining conventional and electric engines in one single aircraft. Hybrid technology leads to extended range compared to all-electric planes and emission of less greenhouse gases than conventional aircraft [18]. Hence many new hybrid research projects were started.

1.1 Problem formulation

The main problem occurring during the design of hybrid aircraft architectures is the optimization of the hybrid system. This relates mainly to how much power of each type is installed or how many energy storage facilities are deployed, correlating to the optimal share of weight for each propulsion system (conventional and electrical in this case). Optimal ranges need to be determined, cost and emission efficient power trains need to be found.

To tackle all these optimization problems, a tool was developed that simulates the hybrid environment of the aircraft and helps to provide the parameters that are used to optimize the propulsion system. This tool will be presented in section 3.

1.2 Outline

In this thesis, the state-of-the-art and technical background of hybrid technology will be presented first. This covers different types of hybrid propulsion systems as well as their pros and cons and the potentials hybrid flying offer. The state-of-the-art of main components in hybrid aircraft is covered (electric engines, gas turbines and batteries). Typical consumers of electrical energy are presented including an estimation of the electrical non-propulsive power consumption of a 19-seater passenger plane. In the end of the first chapter a short overview over promising concept planes is presented. In the second part of the thesis, a simulation tool which was developed as part of the thesis will be explained. The software simulates the energy levels in a hybrid plane and provides detailed metrics about emissions, costs and ranges.

Chapter 2

Background

To start with, the technical background of hybrid flight is presented. Different architectures, advantages/disadvantages and potentials are covered. Subsequently the state-of-the-art of important hybrid flying components like motors, gas turbines and batteries is presented and innovative hybrid or all-electric plane concepts are portrayed.

2.1 Technical background of hybrid planes

2.1.1 Hybrid power trains

2.1.1.1 Types

Hybrid propulsion systems can be divided into two basic types, parallel and serial power trains. In a hybrid aircraft application this relates to whether the shaft power that is driving the propeller is generated by an electric motor or both a gas turbine and an electric motor. This relates to whether power is transmitted electrically or mechanically [23].

In a serial system the thrust-generating shaft is directly powered by an electric motor, power transmission happens solely electrical. In a serial system, a gas turbine and a generator translate chemical power stored as kerosene or other types of fuel into electrical power, which is transmitted via the onboard electrical system to the propulsion motor. This propulsion motor is an electric motor. A battery pack can provide additional electric energy to the system [24]. A diagram for serial hybrid propulsion is shown in Figure [2.1].

If battery packs are the only source of power, Isikveren et al proposed to name this an universally-electric architecture [24]. This type of plane will not be covered much in this work due to its limited range with current battery technology. However, the simulation tool which was developed as part of this thesis features a mode where the range extender can be turned off by setting the input power matrices in an appropriate way. The tool will be presented in Chapter [3] of this thesis.

In a parallel architecture energy is transmitted mechanically to the propulsor-driving motor. This could be done by connecting both an electrical motor and a gas turbine to a shaft to power the propulsor [23]. The gas turbine is directly connected to the shaft (possibly using a gearbox). No energy conversation to electrical energy is done, the shaft is driven only by mechanical energy. A diagram showing the parallel hybrid architecture is presented in Figure [2.2].

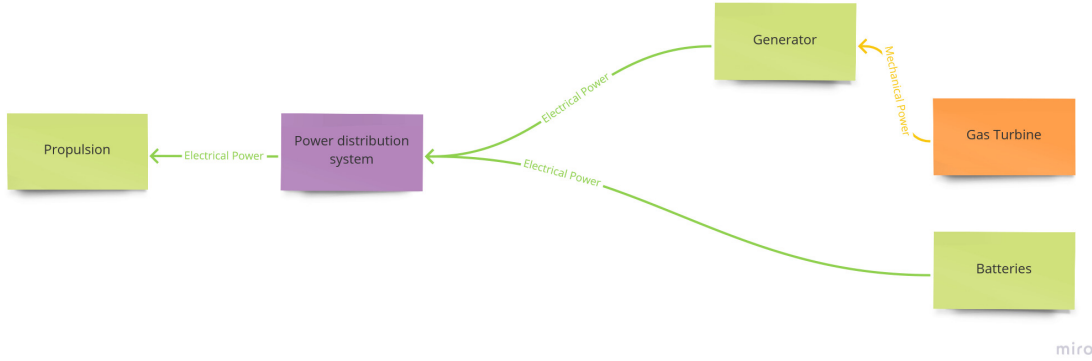


Figure 2.1: Serial architecture according to [1], adapted

Green elements shown in Figure 2.1 and 2.2 are related to electrical power, orange elements symbolize mechanical power transmission by shafts for example. The purple power distribution system refers to the (electrical) power grid of the aircraft.

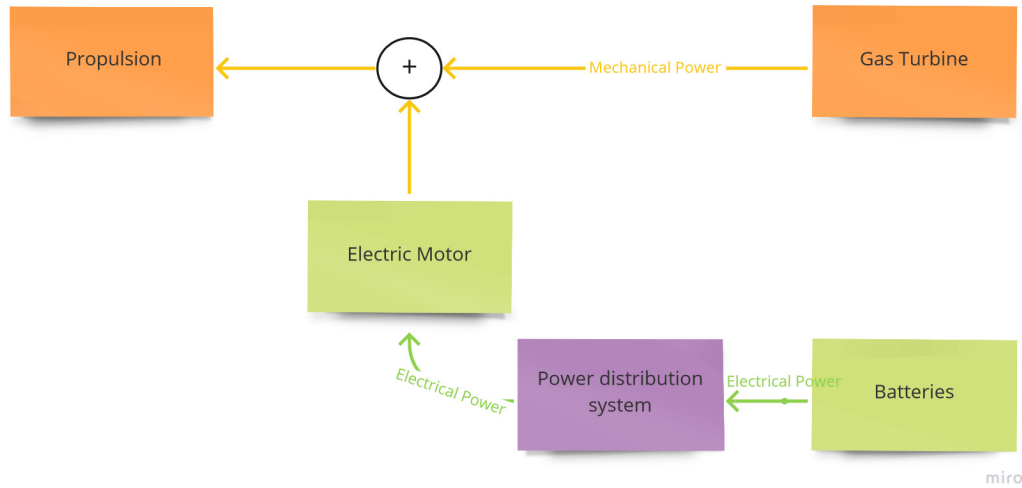


Figure 2.2: Parallel architecture according to [1], adapted

Combinations and derivations of those basic concepts exist as well. A system with various propellers distributed all over the aircraft's wings and skin that are driven all individually by either electrical motors or conventional aircraft engines is called distributed parallel [23].

If the mechanical energy that is provided by a gas turbine is both used to drive the shaft directly but can also be fed into an electrical generator, the system is classified as serial-parallel hybrid [1]

Other hybrid systems exist, but are not further discussed in this work. Which system to choose is related to the general use case of the specific application. Parallel systems could be used for example if the gas turbine runs continuously at its peak power point and the electrical motor supports it during flight segments that require more power than the gas turbine can provide [17]. In most serial systems the turbine works as a range extender and is only turned on if more electrical energy is needed than the batteries can provide. The power transmission there is solely electric.

In general the efficiency of both architectures can be seen as similar but is highly dependant on the application.

2.1.1.2 Advantages

One main advantage of hybrid architecture is its higher efficiency compared to conventional turbo engines [25]. Electrical systems usually have a better efficiency than thermodynamic processes like the Carnot-Cycle [26][27]. In addition, the gas turbine can be run at its peak efficiency point when it is supported by electric motors [23]. The overall efficiency in a hybrid aircraft is nevertheless highly dependant on the share of conventionally generated energy that is provided by gas turbines. It is also advantageous for hybrid planes that the fuel system and infrastructure on the aircraft are already in place and only need to be adapted partially [25].

Hybridification could lead to less noisy aircrafts, but this is highly dependant on the duration electric motors are used during the flight. Using electric motors in take-off and landing segments could decrease the noise significantly [25]. The use of electric motors during certain flight segments depends on whether the electric propulsors and storages can provide enough power during these flight segments. Especially the take-off segments require the biggest amount of power.

Reduction in CO₂ emissions could possibly be achieved as well. This is highly related to whether the battery energy is sourced from renewable energy and the degree of hybridization. The degree of hybridization is an important parameter to classify hybrid aircraft and will be presented in further details in the "Simulation" chapter in section 3.4.3.3

A study designed a concept aircraft with a range of 200 km. This concept aircraft was a 19-seater hybrid-electric aircraft [18]. Paul et al claimed that their designed plane reduces total CO₂ emission by 45,2% with CO₂ intensity for electricity generation in Germany and an efficiency loss due to battery charging of 15% [18]. If the energy used for flying is sourced solely from carbon neutral, renewable energy it is stated to reduce emitted CO₂ by 73,3% [18]. This reduction is calculated for all scheduled planes in this study, assuming that ranges less than 200 kilometres are flown all-electric. In longer flights, the remaining distance is covered by the range extender [18].

These advantages relate to the general concept of hybridization in aircraft applications. The different advantages/disadvantages between the presented architectures above (serial, parallel, etc.) are not covered in this thesis.

2.1.1.3 Disadvantages

Still, some negative aspects of hybrid propulsion systems should be mentioned. Hybrid propulsion systems account for more weight than conventional systems due to heavy battery packs and other equipment to distribute the power in addition to the weight of the conventional propulsion system [25]. More weight leads to more overall energy consumption which relates to reduced range. Range equations quantifying this issue will be presented in 3.4.4.4

Today's battery technology is another factor that is limiting the potential of hybrid flying. Kerosene yields around two magnitudes more usable specific energy (available energy per kg) than battery

packs [25]. The energy density of kerosene is $11.9 \frac{kWh}{kg}$ [28] whereas the energy density of modern batteries is $0.25 \frac{kWh}{kg}$ (see section [2.2.3]). This significant difference leads to much decreased range compared to solely turbo-engine powered aircraft. Even if battery technology advances rapidly, it will not come close to the level of energy provided by kerosene in the next years. The state-of-the-art of the battery subsystem including more details about the energy density will be covered in [2.2.3]. As in hybrid propulsion systems two sources of energy (gas turbine and batteries) are existing, this leads to higher costs managing the energy supply at airports. Kerosene supply infrastructure is available at most airports, but battery charging or replacement infrastructure needs to be established, raising the total costs. This relates to other administrative questions like a unified battery standard for example.

2.1.1.4 Potentials

Despite these disadvantages, hybrid flying has big potential for the future. The share in global greenhouse gas emissions caused by the aviation industry is estimated to be around 4% [19]. In order to tackle global warming, both NASA and related institutions in Europe published guidelines for the aviation industry on how to reduce emissions [29], hybrid planes could be one part of the strategy.

Local hybrid commuter aircraft could also significantly reduce door to door travel time. The German Aerospace Center conducted a study dealing with the potentials of hybrid commuter aircraft [18], which sees improvements in travel time using hybrid commuter planes in certain scenarios.

In addition, hybrid aircraft give designers more freedom in distributing the propulsors all over the aircraft as electrical motors can be much smaller than conventional gas turbines. The power density of electric motors does not scale this much with weight in some extend. This fact will be discussed in more details in the next section [2.2.1] dealing with the state-of-the-art of electric motors. But as smaller motors feature comparable power densities to bigger ones, they could be distributed over the aircraft instead of concentrating the power in big turbo machines.

NASA is currently investigating the potential of a distributed architecture in their Armstrong X-57 Maxwell programme. The concept plane developed in this project will feature 14 electric motors of which 12 are distributed over the leading edges of the wings [23][3]. A deeper look at Maxwell will be given in the Concept Planes subsection [2.3]

2.2 Subsystems

In this section, the state-of-the-art of electrical motors, gas turbines and batteries is presented. Additionally, the biggest energy consumers in aircraft are mentioned.

2.2.1 Electric motors

In hybrid planes, electrical motors replace some or all of the fuel powered motors. Three manufacturers of electrical motors were chosen based on the use of their products in present applications. Their products were expected to have high potential in the future of hybrid and all-electric flying. Some of the power densities are self-calculated and rounded to two decimal places.

2.2.1.1 Siemens/Rolls-Royce

First to mention are the electric motors developed by Siemens' electric propulsion division, which has been sold to Rolls-Royce recently [30]. Therefore a renaming process of certain Siemens products possibly has occurred, nevertheless all products in this section will be named according to their original Siemens' names.

Siemens developed a range of motors in different power classes ranging from 70 kW peak power to 2000 kW. The motor with the most power is the SP2000D. It can provide 2000 kW peak power with a power density of nearly 10 kW/kg and would have been featured in the Airbus E-Fan X (now under new motor name RRP2000D) [31]. The E-Fan X would have been a concept plane where one of four conventional turbo-mechanical engines of the base aircraft would be replaced by an electrical engine. In April 2020 Airbus and Rolls-Royce decided to discontinue the project due to covid-19 [32].

Another electrical motor, the Siemens SP260D motor, is used in Smartflyer planes or the Eviation Alice [33][7] for example. Eviation Alice is a concept plane which will be presented in more details in a following section [2.3] as well.

	SP200D (2017)	SP260D (2015)	SP2000D
P _{max, cont}	204 kW	260 kW	2000 kW
N	1300 RPM non-geared	2500 RPM non-geared	6500 RPM
M _{cont}	1500 Nm	1000 Nm	3000 Nm
U _{DC}	450-850 V	580 V	3000 V
m _{total}	49 kg	50 kg	261 kg
Cooling	oil cooled	oil cooled	direct liquid cooling
Torque to mass ratio	30,6 Nm/kg	20 Nm/kg	11,5 Nm/kg
Power density	4,16 kW/kg	5,2 kW/kg	7,66 kW/kg

Table 2.1: Technical specs of different Siemens motors [7][8]

2.2.1.2 Emrax

Emrax is a Slovenian company focusing on manufacturing axial flux e-motors for aviation applications. Their motors' maximum power outputs are slightly below those of the Siemens motors but the power density of their products is close to 10 kW/kg. Further insight data can be found in table [2.2] below. Two motors can be stacked together to double the available power and torque. This feature provides fast customizable solutions for different motor demands [34]. Emrax motors are mostly used in smaller glider or flight education aircraft [34]. They could also be used well in a distributed propulsion setup.

2.2.1.3 MagniX

MagniX is a US-/Australian-based company developing electric motors and corresponding controllers [40]. Their products can be used in similar applications like the Siemens motors, their website claims that the magni250 motor is also used in the Eviation Alice (so it is comparable to the SP260D motor which is also used in Alice). The more powerful magni500 motor is used for "Middle-Mile" aircraft like the Cessna Caravan [9].

	Emrax-188 [35]	Emrax-208 [36]	Emrax-228 [37]	Emrax-268 [38]	Emrax-348 [39]
P _{max, peak}	52 kW	68 kW	109 kW	200 kW	380 kW (low voltage)
N	6500 RPM	6000 RPM	5500 RPM	4500 RPM	4000 RPM
M _{max}	90 Nm	140 Nm	230 Nm	500 Nm	1000 Nm
U _{DC}	430-110 V	550-120 V	680-160 V	800-250 V	800-420 V
m _{total}	7,0-7,3 kg	9,1-9,4 kg	12,0-12,4 kg	20,0-20,5 kg	41-42 kg
M/m (best case)	12,86 Nm/kg	15,38 Nm/kg	19,17 Nm/kg	25 Nm/kg	24,39 Nm/kg
P/m (best case)	7,42 kW/kg	7,47 kW/kg	9,08 kW/kg	10 kW/kg	9,27 kW/kg

Table 2.2: Technical specs of different Emrax motors; due to different submodel types only the general data for each model is given; ratios self calculated; best case values were used for calculation

	magni250	magni500
P _{cont}	280 kW	560 kW
N _{max}	3000 RPM	2600 RPM
M _{cont}	1407 Nm	2814 Nm
U _{DC, nominal}	540 V	540 V
m _{total}	71 kg	133 kg
Efficiency	> 93%	> 93%
Torque to mass ratio	19,82 Nm/kg	21,16 Nm/kg
Power density	3,94 kW/kg	4,21 kW/kg

Table 2.3: Technical specs of MagniX motors [9]; ratios self calculated

2.2.1.4 Comparison

All three presented companies offer interesting products. The products of Siemens and Emrax are quite similar with regard to the provided torque to mass ratio and power density. The differences here are caused by the different rotation speeds of the motors

MagniX motors are a lot heavier than the other motors, but the provided (specific) torque is comparable to the torque provided by the Siemens motors. Therefore Siemens engines would be the better choice regarding mass only.

Emrax motors provide the highest power density. Most of the presented motors are not powerful enough to compete with bigger conventional aircraft engines. Small aircraft engines have high power outputs which are at least comparable to the power outputs of the gas turbines presented in the next section [2.2.2]. Nevertheless the newly developed SP2000D engine could be a candidate to replace small engine units in aircraft with its outstanding 2 MW of continuous power. The other motors presented in this section could be well used in a distributed setup, especially the Emrax products. Which motor to choose is depending on the required power density, specific torque and the rotation speed.

2.2.2 Gas turbines

Current battery technology cannot provide sufficient energy to fly longer distances. In the study [18] it was assumed that state-of-the-art electric/hybrid planes could fly 200 km with an additional diversion reserve powered solely by electrical power. Therefore gas turbines are used as an additional

source of energy to extend the range of hybrid aircraft.

The gas turbines, which are best to use in hybrid planes, are turboshaft engines. Turboshaft engines are designed to produce shaft power instead of thrust, which is normally generated in conventional plane engines [41]. The power shaft can be connected to the propeller directly (sometimes with a gearbox in-between) or to a generator to generate electrical power, again depending on the chosen hybrid architecture. Turboshaft engines are often used in helicopters.

One main advantage of using gas turbines connected to a generator is the spacial flexibility. In this case the propulsion itself is solely electrical. Electrical power can be generated elsewhere in the aircraft by the gas turbine and is distributed to the propulsors via the onboard electrical network. The gas turbine could be located in the fuselage and does not necessarily need to be placed in a nacelle under the wing, which reduces drag. This was done in concept studies like [42][43] for example. In addition the generator in the Airbus E-Fan X would have been located in the fuselage [44].

In this section three big suppliers of gas turbines and their products are presented. The companies were chosen as examples for the state-of-the-art. There are many more companies manufacturing gas turbines in the same power section. The power densities were calculated with the maximum continuous power. The results were rounded to two decimal places.

2.2.2.1 Safran

Safran is a French aerospace company manufacturing product families ranging from aerospace engines to cabin interior [45]. Three medium sized gas turbine product families were chosen and will be presented below. In some of these families only the most powerful engines will be presented to give an overview over the state-of-the-art.

Arrano Arrano engines feature a two-stage centrifugal compressor and a reverse flow combustion chamber [10], its data can be found in Table 2.4

Ardiden The Ardiden family features many designs of the Arrano series, for example the two-stage centrifugal compressor and a reverse flow combustion chamber. Nevertheless the power these units can provide is higher but they also account for more weight [11]. The data of the Ardiden engines can be found in table 2.5.

Ardiden engines will be used in Zunum Aero aircraft as part of their hybrid propulsion system [46]. Zunum Aero is a hybrid aircraft which is currently developed by Zunum. Zunum is facing financial problems therefore the project could be discontinued in the future.

MTR390-E This engine is developed jointly by Safran, Rolls Royce, MTU and ITP Aero. The developers state that it will be the most advanced turboshaft engine of its class, providing more power than the previous model with the same architecture and installation envelope [12]. Its data can be found in table 2.6

	Arrano 1A
m_{dry}	175,1 kg
$P_{All \ engines \ operative \ (AEO), \ max, \ cont}$	738 kW
$P_{AEO, \ take-off}$	851 kW
Power density	4,21 kW/kg

Table 2.4: Technical specs of Arrano [10]

	Ardiden 3G	Ardiden 3C
m_{dry}	215 kg	226,6 kg
$P_{AEO, \ max, \ cont}$	913 kW	902 kW
$P_{AEO, \ take-off}$	1177 kW	968 kW
Power density	4,25 kW/kg	3,98 kW/kg

Table 2.5: Technical specs of Ardiden family models [11]

	MTR390-E
m_{dry}	179 kg
$P_{AEO, \ max, \ cont}$	995 kW
$P_{AEO, \ take-off}$	1322 kW
Power density	5,56 kW/kg

Table 2.6: Technical specs of MTR390-E [12]

2.2.2.2 General Electric

General Electric's (GE) gas turbine family is the CT7/T700 family. The engine unit is used in a variety of helicopters, both in civil and military aviation. In this work, the military versions are presented in table 2.7 due to better data availability. The civil engine units are comparable to the military ones. Sources are cited in the table.

2.2.2.3 Rolls-Royce

Rolls-Royce is well known for its aircraft and helicopter engines. Two gas turbines will be presented, one of those is manufactured by a Joint-Venture of Rolls-Royce and Honeywell. This engine is called CTS800 [51].

CTS800 [51] This engine is a collaborative project of Rolls-Royce and Honeywell. It was used for example in Lynx helicopters. The technical features are quite similar to the Safran engines, a two-stage centrifugal compressor and a reverse-flow combustion chamber are integrated [13]. Data can be found in table 2.8.

AE2100 Although the AE2100 unit is a turboprop engine, it is mentioned here, because derivatives of it exist as turboshaft variants. As stated in [11] both engine types are quite similar. The technical

T700	-401C [47]	-701D [48]	-701K [49]	/T6A1 [50]
m_{dry}	208 kg	207 kg	228 kg	224 kg
$P_{AEO, \text{max, cont}}$	1239 kW	1279 kW	1228 kW	1394 kW
$P_{AEO, \text{take-off}}$	1409 kW	1491 kW	1325 kW	<i>no data available</i>
Power density	5,96 kW/kg	6,18 kW/kg	5,39 kW/kg	6,22 kW/kg

Table 2.7: Technical specs of T700 family models

data will be roughly the same for the turboshaft variant. Its technical specs can be found in table 2.9

	CTS800-4N
m_{dry}	185,1 kg
$P_{AEO, \text{max, cont}}$	955 kW
$P_{AEO, \text{take-off}}$	1014 kW
Power density	5,16 kW/kg

Table 2.8: Technical specs of CTS800-4N [13]

	AE-2100D2
m_{basic}	783 kg
$P_{AEO, \text{max}}$	3458 kW
Power density	4,42 kW/kg

Table 2.9: Technical specs of AE-2100D2 [14]

2.2.2.4 Comparison

Which gas turbine to choose in a hybrid application depends on various parameters, for example the intended range, the maximum take-off weight of the plane, the energy and power demands of the plane and the chosen hybrid architecture. Basically the aim in designing hybrid aircraft is to provide the best range with the smallest amount of non-electrical energy possible as electric propulsion leads to less in-flight emissions (CO₂, noise). This is non-electrical energy generated by gas turbines using kerosene.

Generally, all types of engines could be used in hybrid applications, relating to the required amount of energy. The Smartflyer for example uses a Rotax engine as a range extender [7]. The focus in this work are turboshaft gas turbines, because they are lightweight engines with high efficiencies [41]. All the gas turbines presented feature power densities between 4,0 kW/kg and 6,0 kW/kg. The highest power density is provided by the T700-T6A1 with 6,22 kW/kg.

2.2.3 Batteries

Batteries are the second main source of energy in a hybrid aircraft and the most crucial factor limiting the performance of hybrid aircraft. In this section the theoretical background of batteries and

problems occurring using batteries as main power source are presented. Later on two manufactures of battery systems are portrayed.

2.2.3.1 Theory and problems

The key parameter to compare batteries is the gravimetric density which is calculated by dividing the total energy content by the total mass of the battery. Mass is a crucial factor in aerial applications because higher mass leads to higher power consumption.

Conventional planes loose mass during flight because kerosene is burnt in the motors. In contrast, electrical components like batteries do not change their weight while discharging. Therefore the battery size needs to be perfectly adapted to the use case of the plane, otherwise the aircraft's efficiency is declining.

Current state-of-the-art commercial batteries feature a gravimetric density of 200-255 Wh/kg [20][23]. Extensive research is done to improve gravimetric density of batteries. Statistically the energy density increases by 7 % every year [52].

Today's electrode materials, which is often lithium, limit the gravimetric density below 300 Wh/kg [52], but predictions say that energy densities of 1500 Wh/kg will be achievable by 2035 by using new materials [52].

In comparison, kerosene yields an energy density of 11,9 kWh/kg [28]. A rise in battery energy density can only be achieved by using new electrode materials or technologies like Lithium-Air or Lithium-Sulfur batteries [23][53]. Those technologies can theoretically achieve much higher densities [53] but are still far away from commercial application. At the moment, battery energy density is the biggest factor limiting range of electric aircraft as batteries have a much smaller energy density than kerosene [25].

Besides the gravimetric density, the number of charging cycles is also important, as less cycles lead to higher costs, since the battery needs to be replaced more often. Hoelzen et al state that 1500 cycles can be achieved in future battery applications [53]. Current batteries for cars and planes can be charged around 1000 times [20]. The BorgWarner battery pack presented below even achieves 3000 charging cycles [16].

Modern lithium based batteries rose controversy as rare earth elements are used for manufacturing of these batteries. These rare earth elements are related to modern slavery and environmental pollution [54][55]. These problems should be mentioned as well but will not be covered in more detail.

2.2.3.2 KOKAM

KOKAM is a supplier of lithium-ion battery technology founded in South Korea in 1989 [56]. They offer battery systems for a wide range of applications including aviation, electric vehicles, and submarines. Their SLPB080085270 cell features the companies' highest power density with 248 Wh/kg [57] at cell level. These cells are used in their Ultra High Energy Pack (UHE), which is designed for aviation applications, for details look at table 2.10

The presented pack is close to the maximum current state-of-the-art with its 220 Wh/kg energy density. Another KOKAM battery system even provides 255 Wh/kg and this system is used in Eviation Alice [20]. The implementation details and technical specs of this system in Alice remain unclear.

Model name/ used cells	SLPB065070180	SLPB080085270
Cell capacity	11,6 Ah / 255,2 Wh	26 Ah / 572 Wh
Nominal voltage	22 V	22 V
Max Charge	11,6 A	26 A
Max Discharge	2 C	2 C
Peak Discharge	4 C	4 C
Weight	1,2 kg	2,6 kg
Energy Density	212,67 Wh/kg	220 Wh/kg

Table 2.10: Technical data of KOKAM UHE Pack [15]

2.2.3.3 BorgWarner

BorgWarner is a US-based automotive supplier. It mainly manufactures conventional automotive technology, but also features hybrid/electric drive components. Their electric product portfolio ranges from electric drive motors and power electronics to battery systems [58]. Their battery system that was designed for automotive applications in electric cars will be presented below.

The battery system is called Hermes. It features a thermal management system ready for active and passive cooling and an intelligent battery management algorithm. BorgWarner claims that the pack can be charged more than 3000 times [16].

	Hermes
Cell capacity	10 kWh
Nominal voltage	40 V to 67,2 V
Continuous charge	1 C
Continuous discharge	1,5 C
Weight	48 kg
Energy Density	208,34 Wh/kg

Table 2.11: Technical data of Hermes battery system [16]

This battery pack has a slightly smaller energy density than the KOKAM one presented above. Nevertheless it features interesting technical specs, for example voltage provided by the BorgWarner system is higher than voltage provided by the KOKAM pack.

2.2.3.4 Summary

The two presented battery systems are examples to provide an insight into the state-of-the-art of batteries. Nevertheless they might not be the ones with the highest energy density. In comparison, the battery system used in a Tesla Model S only has a much lower gravimetric energy density of 137,5 Wh/kg [59].

Battery cells are the core components of battery systems. In these systems cells are connected together in parallel and in series while being monitored by other electronic components to ensure battery safety, performance and life. These added parts account for the lower gravimetric energy

density of the whole system as their weight is useless for energy storage but added to the total weight of the system. The individual cells can feature a much higher energy density. For example the NCR18650A cell, which was used by Tesla previously, has an energy density of 251,69 Wh/kg [60]. This cell was released in 2009. The cell's energy density is close to current battery system energy density, which makes the difference between cell level and system level quite obvious. As energy densities will rise and cell prices will probably decrease in the future due to higher demand and better manufacturing technology, electric and hybrid applications will become more interesting and applicable.

2.2.4 Electrical loads

Various systems in modern aircraft consume electrical energy, avionic equipment, lighting and passenger-related systems like in-flight entertainment or galleys for instance. In this section an overview over the different existing systems will be given. Moir et al divided the main electrical loads into four main categories; motor and actuation, lighting services, heating services and subsystem controllers and avionic systems [61]. All of these require different levels of power, continuity of electrical energy and quality (high-conditioned energy vs unconditioned energy). Some of them are necessary to fly whereas other serve needs of comfort. Much information presented in this chapter and its subchapters is taken from the book [61], other sources are cited.

2.2.4.1 Motor and actuation

In conventional aircraft, linear motors are used for controlling the engines and the flight control systems (trim actuators) or to control valves of many subsystems like the hydraulics, the fuel system or air control. These systems often feature pumps which mostly consume electrical power. Other motors are used as start engines, gyroscope motors or cooling fan motors. Not all of these motors are used continuously. Cooling fans and gyroscope motors need to run all the time to ensure functionality of the plane whereas starting or flight control motors are only used during certain phases of the flight.

2.2.4.2 Lighting services

Lighting can be found all over the plane, both internal and external. External lights are mostly for flight safety, like landing lights, navigation lights or emergency evacuation lights, to name some. Internal lighting equipment is used to light the equipment panel in the cockpit and passenger section (general/personal lighting, emergency lights) for instance. Filament bulbs are often installed, which consume from 600 W for landing lights to tens of watts for smaller interior applications.

2.2.4.3 Heating services

Heating requires vast amounts of energy which is mostly electric. Heating service devices are used for de-icing of wings or windscreen heating for example. Besides the heating devices itself, controllers to time, cycle and switch the state of the heater are required, as well as thermometers [61]. Electrical heaters consume up to tens of kilowatts. Fortunately, this power is not required to be frequency stable and is therefore relatively easy to generate. Nevertheless, heating is very energy-intensive.

2.2.4.4 Subsystem controllers and avionic systems

Avionic systems are very important, they are used in navigation or communication for instance. Most of those have small power loads, but are crucial for a safe operation of the plane and therefore need a continuous power supply.

Therefore it needs to be ensured that there is power available during the whole flight for critical systems, even in case of an emergency.

2.2.4.5 Ancillary systems

Some systems are not needed for safe aviation. They could either be installed for reasons of comfort or need to be installed due to design requirements of the airlines.

Pressurization is needed to fly above a certain altitude. But in shorter flights you can stay below this altitude to avoid pressurization [17]. This saves power and leads to less strains to the fuselage. In-flight entertainment systems and galleys mainly serve passengers' comfort and are not essential, so it could be discussed whether a particular ancillary system is needed in the aircraft. Whereas in-flight entertainment does not consume much power, galleys are assumed to consume up to 10 kW of power.

2.2.4.6 Summary

Besides the electrical system other sources of power transmission exist in conventional planes like hydraulic power or bleed air. It is likely that in hybrid aircraft some or all of these other power sources disappear and all subsystems are powered by electric power. This reduces unnecessary system redundancy.

Systems like conventional environmental control (pressurization) require bleed air. Bleed air is compressed air, which is generated in turbines as part of the combustion process. As turbines might not be active during the whole flight in hybrid aircraft, an alternative needs to be found.

In addition, some systems included in present conventional aircraft might not be necessary. The first hybrid aircraft entering the market will likely not fly long ranges. Galleys to serve hot meals during flight are probably not useful on a two hour trip and in-flight entertainment could be replaced by on-demand services that can be used on personal devices. Avoiding unnecessary systems saves weight and reduces electrical loads.

Electrical motors and actuators could replace the state-of-the-art of moving the flight control surfaces with hydraulic power. This is already done in more-electric aircraft (MEA) like the new Airbus A320 and Boeing 787 where actuators move the flight control surfaces [62].

The A320 only consumes 50 kW of electrical power in total, the 787 can produce 1000 kW at maximum [62]. Conventional aircraft like the A330 have an installed electrical capacity of 300 kW, which is around 13% of the non-propulsive power. Other MEAs like the A380 feature up to 600 kW installed electrical power [1].

It is hard to estimate how much electrical power will be consumed in a hybrid plane with 19 passengers due to the uncertainty of built-in systems and the fact that 19 seater aircraft are a niche market with around ten percent of all active planes [18] [63]. Therefore not much data is available. Xia et al describe the energy consumption of a 130-seater plane in [64]. There it is stated that the maximum summed power requirement to power all systems is 275,6 kW. This data was taken to extrapolate the power consumption of a 19-seater aircraft.

With the provided data an overall power consumption of a 19-seater plane without kitchen equipment

was estimated based on Appendix A in [64]. This leads to an overall cruise load between 100 kW and 150 kW.

2.3 Concept planes

In this section four interesting concept planes will be presented. Some of them are intended to just be proof-of-concept platforms like Rolls-Royce ACCEL, others try to enter the commercial aircraft market in the mid 2020-th. Not all of them are hybrid planes but some are equipped with all-electric propulsion systems. Nevertheless, the technology these plane feature is beneficial for hybrid aviation because the long-term aim of hybrid aviation should be to switch to all-electric propulsion.

2.3.1 Eviation Alice

Eviation is an Israeli startup which is developing the Alice aircraft. Alice is an all-electric propulsion aircraft with 9 seats (plus two crew seats) which is expected to enter into service in 2022 [22]. It features a range of 540 nautical miles with 45 min reserve. Its powerplant can provide 900 kW peak power and 260 kW in cruise. Siemens SP260 motors are used [33]. The built-in lithium-ion (NMC) battery has a capacity of 920 kWh and weighs 3600 kg which is around 60% of the maximum take-off weight (MTOW). The battery cells are provided by KOKAM (see section 2.2.3.2 above) and have a power density of 255 Wh/kg. The charging of the batteries takes 30-70 minutes and 1000 charging cycles can be done which relates to 3000 flight hours [20]. The maximum take-off weight (MTOW) is 6350 kg. The company claims that Alice offers direct operating costs of 200 \$ per hour only, which is less than conventional planes offer [20]. A picture of Alice is shown in Figure 2.3



Figure 2.3: Eviation Alice at Paris Airshow 2019; taken from [2]

2.3.2 X57 Maxwell

X57 Maxwell is the first experimental all-electric aircraft NASA launches [3]. Maxwell is based on an Italian Tecnam P2006T that will be retrofitted with an electric propulsion system. It will be built with carbon fibre composite material [65]. If not otherwise indicated, all information in this subsection will be cited from [3].

The project is divided into 4 (modification) phases, the final configuration will feature 14 electrical

motors spread over the wing tips. Two motors will provide main thrust during cruise, the other 12 generate lift. A special smaller wing form will be used which makes this configuration necessary. Overall, this design will improve efficiency. This design is a great proof of concept of distributed propulsion systems. If the concept succeeds, this could be a leading example for future hybrid distributed propulsion systems.

In the first phase called LEAPTech the propulsion technology was validated and flight data of the plane was collected. In the second phase, besides more testing the aircraft was turned into an electric one by replacing the two turbines with electrical motors. Phases three and four will take the aircraft into its final configuration. In its final state all motors are activated during take-off, during cruise only the two cruise motors remain activated. The lift motors can be folded into the nacelles to reduce drag during cruise. Overall, the aircraft is stated to be up to 500 percent more efficient than conventional aircraft at cruising speed [65]. A picture of X57 Maxwell is shown in Figure 2.4



Figure 2.4: Computer-simulated figure of X-57 concept; taken from [3]

m	1360 kg
P _{cruise, single motor}	60 kW
P _{lift, single motor}	10,5 kW
m _{batteries}	390 kg
E _{battery, usable}	47 kWh
Power density _{batteries}	120,51 Wh/kg

Table 2.12: Technical specs of X57 Maxwell in final configuration [3]

2.3.3 Rolls-Royce ACCEL

During the ACCEL project, Rolls-Royce is aiming to develop the world's fastest all-electric plane together with partners [66] [67]. The aircraft is scheduled to fly in 2020. Only one seat will be used in the aircraft; nevertheless it demonstrates the current state-of-the-art in an impressive way, therefore it is featured in this work. The plane is based on a Nemesis NXT aircraft with a range of

170 NM [67] which is roughly 320 km. Three lightweight YASA 750 R motors installed in series will be used providing a maximum power of 750 kW. MTOW is 1200 kg. The speed of the aircraft should be at least 481 Km/h [67]. The used powertrain will be run at 750 V with 90 percent efficiency [66]. Three battery packs will be installed, each consisting of 6000 cells [68]. One battery pack will provide 72 kWh and weighs 450 kg. This leads to an energy density of 160 Wh/kg. It is stated that this energy density is similar to a Tesla Model 3's, but in order to be able to compete with normal fuel, at least 500 Wh/kg are needed [68]. The main challenge seems to be the cooling system [68], because dense battery packs produce a not negligible amount of waste heat. A picture of ACCEL is shown in Figure 2.5.



Figure 2.5: ACCEL; taken from [4]

2.3.4 Ampaire 337

Retrofitting a Cessna 337 Skymaster to equip it with a hybrid propulsion system is done in the Ampaire 337 project. The six-seater plane is being developed by the US-american startup Ampaire [69]. The Cessna is equipped with both an electrical propulsion system and a conventional fuel based system, both working independently of each other [70]. One propeller is located in the front of the aircraft whereas the other one is placed in the back. Charging of the batteries during flight is not possible. The electric propulsion system features a 160 kW motor and adds around 180 kg to the certified mass of the base aircraft. The jet fuel propulsion system stays unaffected because the factory engine is used.

The batteries need to be recharged or changed after flight [70]; charging takes around 2 hours, a change of the batteries can be done in 15 minutes in the final configuration. The company states that the electric powertrain's noise is 85 percent reduced compared to the replaced conventional one [70]. A picture of Ampaire 337 is shown in Figure 2.6.

2.3.5 Summary

All presented planes provide a great demonstration of the state-of-the-art, independently from their future commercial usability. These projects support the change from conventional propulsion to



Figure 2.6: Ampaire 337 concept plane; taken from [\[5\]](#)

hybrid propulsion and provide useful data for future projects.

There is a market for small hybrid planes in the near future [\[18\]](#) and hybridization of bigger medium-range aircraft could be achievable in several decades when the battery technology advances to power densities comparable to fuels. Despite the corona-crisis which made some companies to discontinue their hybrid aircraft projects, there are more projects dealing with hybrid propulsion than the four presented here.

Chapter 3

Simulation

One primary part of the thesis was to develop a tool to simulate the powergrid of a hybrid aircraft. The developed tool simulates the energy levels of the batteries and fuel tanks and provides some additional descriptive parameters of the plane. Most parts of the tool can be used within the graphical user interface (GUI) of the tool.

3.1 Outlook

Firstly an overview over the structure of the code will be provided in section 3.2. The contents of the five simulation files will be explained including a description how to run the tool.

In the next subsection 3.3 the features of the software and their implementations are covered. The fundamentals of the energy level simulation and the modelling of the propulsion system are presented.

In section 3.4 the metrics and parameters shown in the four GUI windows are displayed including their theoretical background. In the end in section 3.5 simulation results for a 19-seater hybrid aircraft are presented to give an example for the use-case of the tool.

3.2 Structure

The simulation tool was written in Octave 4.4.0 using mainly MatLab syntax. Therefore it runs both in Octave and Matlab, although some features are not supported in MatLab. The tool was not tested using MatLab. It is recommended to use Octave 4.4.0 to run the tool, the version the tool was developed with.

The tool is divided into five files called Simulation.m, updateGUI.m, writeInput.m, calculateMeasures.m and calculateMetrics.m. To run the software, all five modules need to be located in the same directory, but only Simulation.m needs to be opened in Octave. Simulation.m works as a main function and needs to be run to start the simulation. Running the software will open four individual windows. The content of the four windows will be explained in a following section. A schematic of the tool architecture can be seen in Figure 3.1. The tool comes ready to run with initial values set describing a 19-seater plane (see Section 3.5.1 for more information).

In addition to this thesis text, the code is well-commented and combining both should give a good

understanding. The code is not presented in this text but implementation details and theoretical backgrounds are covered.

3.2.1 Running the simulation

Simulation.m needs to be run in Octave to open the simulation environment. After launch of the tool, the main simulation is started by pressing "SIMULATE" in the "Main GUI" window which opens after running the tool in Octave. It may occur that the other three windows are displayed over this window, in this case move the other windows on your screen.

Once the simulation is carried out, a plot appears (if the input values describe a valid aircraft environment) in the window and the "Executed" LED changes its colour, depending on a successful execution.

More detailed metrics can be acquired by pressing the "Calculate" buttons in the "Insights" and "Metrics" windows. The parameters calculated in "Metrics" depend partially on the values calculated in the "Insights" figure. Therefore the "Insights" computation needs to be run at least once before any calculation in "Metrics" can be done.

Editing values is not affected by this initialization issue, editing in any GUI frame can be done right after launch. After an initial run Octave saves the values until they are cleared, overwritten or Octave is restarted.

The calculated metrics will be presented in further details later in the "Insights" [3.4.3](#) and "Metrics" [3.4.4](#) subsection.

The features of the other buttons will be covered as well in their corresponding subsection, but their tasks are mostly self-explaining.

The maximization of windows led to big delays while using the software during development of the GUI, so it is not recommended to maximize any windows in Octave. It seems to be an issue with the uicontrol package that was used to design the GUI.

Units of input values are given in brackets behind the corresponding label in the GUI.

Following, structure and purposes of the individual files are explained.

3.2.2 Simulation.m file

This file serves as the main function of the tool. In the first part all relevant global variables are initialized with values that describe a 19-seater aircraft. The composition and sources of these values are discussed later in the "Validation and Simulation Results" section [3.5](#).

In the next part of the simulation.m file, all GUI elements are initialized and placed into the corresponding figures. The uicontrol MatLab/Octave package was used to design and develop the software/GUI. The most used properties are textboxes, editable labels and push-buttons. Their callback functions are located in the other four files. These callback functions are called when an interaction with the UI-elements occurs. For more information about the usage of the uicontrol package, read the documentation found here [\[71\]](#) [\[72\]](#).

3.2.3 writeInput.m file

writeInput.m provides the functionality to the GUI elements on the second window named "Input Variables", which are introduced in Simulation.m, beginning at line 124 going to line 203. Every time a value is written into one of the boxes in the second frame "Input Values" of the interface, the callback function assigned to each element is called. This callback function is called "writeInput",

which is located in the writeInput.m file. It overwrites the corresponding global value with the new provided one in the input box. This rewritable boxes are used in all frames of the GUI and work in the same way.

3.2.4 updateGUI.m file

This file provides functionality to the "Main GUI" window. It handles interactions with the buttons and checkboxes defined in Simulation.m line 80 to 121 as well as writing new values corresponding to the threshold. The main simulation computation also happens in this file. The calculation will be displayed in more details in section 3.4 below.

3.2.5 computeMetrics.m and computeMeasures.m files

Both files serve similar purposes, they provide more detailed figures of merit. Calculation of these metrics is done and results are displayed. Many metrics need more parameters of the simulated plane to be able to be calculated, input boxes for those required parameters are handled by the files/functions as well. The GUI element initialization for computeMeasures.m start at line 206 in simulation.m and for computeMetrics.m at line 270.

Figure 3.1 displays the tool architecture.

3.3 Simulation details

The hybrid plane simulated here is not specified in its hybrid architecture presented in section 2.1.1. As only the chemical and electrical power drains and sources are provided as input parameters and the main source of shaft power remains undefined, a commitment to one particular architecture is not needed.

The closest and most intuitive architecture this tool simulates is a distributed parallel architecture presented by Pernet [23]. Aircraft using distributed parallel architectures would feature both conventional gas turbines and electrical motors installed independently of each other [23]. This concept reduces complexity as for example conventional and electrical power units do not need to be connected together to one shaft [23].

3.3.1 Input matrices

The general simulation objective of the tool was to model the energy consumption/levels of a hybrid plane during flight in all three flight phases (take-off, cruise, landing) and the corresponding energy levels in the batteries and fuel tanks. Therefore the most important input parameters were the provided power by batteries and gas turbines/engines as well as the electrical and chemical (stored as fuel) power consumption used for thrust.

To store these input values in a convenient and compact way, a matrix system was introduced. A matrix was assigned to each flight phase, making it possible to have different power requirements in each phase. The matrices are called T for take-off, C for cruise and L for landing.

3.3.1.1 Matrix format

All input matrices are 3x3 matrices and are based on the same format presented here. To describe the content of the matrices, MatLab indexing will be used in this thesis. Further information about

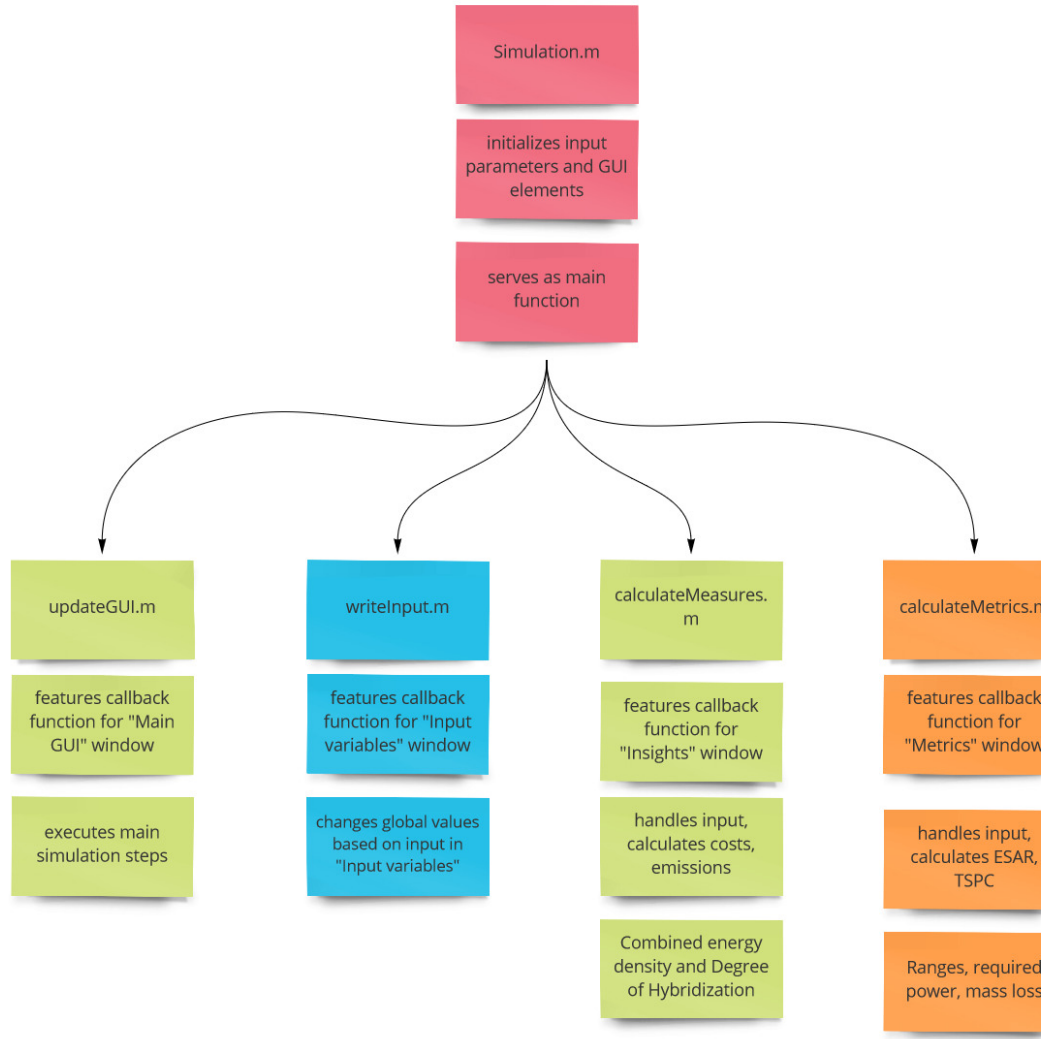


Figure 3.1: Architecture of the simulation tool

MatLab indexing can be found in the documentation [73].

Value (1,1) of any input matrix refers to the duration of the particular flight phase in seconds. The second line describes the provided power by batteries and fuel in kW. Value (2,1) hence relates to the available electrical power (batteries) and value (2,2) to the available chemical power (fuel). This provided power can either be seen as the maximum of power the engines can supply or the amount of energy that can be delivered by fuel or batteries in a certain time, so relating to the onboard electrical distribution system and the fuel pump system. In this thesis it describes the

distribution capacity of the electrical distribution system and the fuel pumps.

The third line characterizes the (thrust) power in kW. Normally thrust is given in Newton N. In this thesis, as thrust is generated by the engines using power, power is used to describe the amount of generated thrust. Thrust and power are intertwined by the velocity. So sometimes in this work, thrust, power and energy are used interchangeably as they all describe the same thing, the energy levels in batteries and fuel tanks.

Value (3,1) describes the thrust power generated by the installed electrical motors, value (3,2) the thrust power requirements of installed fuel powered motors. These two values describe the actual amount of thrust in kW that is used in the end. To obtain the amount of power drained from the onboard power distribution systems (electrical and fuel), these parameters need to be divided by the efficiencies of the corresponding propulsion system. The last value (3,3) refers to power consumed by all other electrical systems like avionics or cabin equipment. All consumptions are adjusted by the efficiencies of their power source, so values (3,1) and (3,3) are adjusted by the efficiency of the electric propulsion system (eps_effi); value (3,2) is adjusted by the efficiency of the conventional propulsion system (turbine_eff).

All matrix entries are assumed to be constant during each flight phase. This is only an approximation to any real aircraft as power consumption changes over time due to changes in weight for example. Matrices containing values changing over time could be implemented in a future version.

Nevertheless the tool provides an overview over the required power and aircraft weight and their change over time in the "Metrics" window. These changes are not affecting the values in the matrices or in the basic energy level simulation at the moment.

Other matrix entries than the presented ones are not used in the simulation. For better understanding of the matrix format, look at the example below.

Example Given matrix E
$$\begin{pmatrix} 450 & 0 & 0 \\ 1000 & 950 & 0 \\ 700 & 250 & 100 \end{pmatrix}$$
 as an example. The matrix describes a flight phase

which has a duration of 450 seconds (first line).

1000 kW of electrical power are provided by the batteries and 950 kW of chemical power are provided by the fuel pump system during this phase (second line).

700 kW of electrical power are drained unadjusted by the electrical propulsion system as thrust, 100 kW by all other electrical power consumers in the aircraft. 250 kW of thrust power are consumed by the conventional propulsion system. The efficiency of the conventional propulsion system was set to 0.3 and to 0.8 for the electric propulsion system.

This leads to more chemical power supplied than used ($950 - (250/0.3) = 116$), 116 kW are unused during the whole flight phase after the conversation efficiency of 0.3 was applied. These 116 kW are converted into electrical energy with an efficiency of eff_fuel2el and added to the balance of electrical energy.

3.3.2 Energy storage/propulsion systems modelling

The modelling of the battery is based on the battery weight (b_weight in the code) in kg, the battery capacity ($b_capacity$ in the code) in kWh and the state-of-charge (SOC, also the same name in the code) of the battery as a percentage (0-1). Additionally, the battery capacity describes the usable capacity ($b_capacity$), so any energy losses during charge/discharge or use are already calculated into the capacity, $usable_batt$ refers to the total available usable power. The SOC is

multiplied with the battery capacity at the start of the simulation to obtain the initial usable energy during flight. This is a simplification as other losses are not taken into account. An efficiency for converting the usable energy into thrust is introduced in the tool called `eps_effi`. This efficiency refers to the overall efficiency of the electric propulsion system and will be used for other metrics as well. As described previously, the thrust power generated by the engines defined in the matrices is divided by this efficiency to obtain the actually drained power from the electrical power distribution system.

Modelling of the conventional propulsion system is similar to the modelling of the electric system. Usable energy (`fuel_energy` in code, energy content of all loaded kerosene) in kWh is provided as well as the kerosene weight (`kerosene_weight`) in kg and the efficiency of the conventional propulsion system (`turbine_eff`) as a value between 0 and 1, which describes the conversation efficiency from fuel energy to thrust. Kerosene weight is calculated based on the energy density of kerosene (11.9 $\frac{kWh}{kg}$ [28]) and the turbine efficiency. Usable fuel energy describes all energy that can actually be used for flying already including all energy losses.

3.3.3 Basic simulation

The basic calculations to be able to display the plot in the "Main GUI" window and simulate the energy levels are done in `updateGUI.m` beginning in line 156. The calculation is done for each flight phase individually. The calculation algorithm looks like this:

1. The calculation is carried out in intervals, the duration of these intervals is defined in `time_step` in the code, initially set to 0.5 seconds. After every interval, the simulation steps are done. Therefore the number of calculations to be done is computed first by dividing the duration of the particular flight phase stored in the matrix value (1,1) by the `time_step` defined in the "Metrics" window. After that, the total electrical power drain is calculated $\frac{(3,1)+(3,2)}{eps_effi}$. The total electrical power drain is adjusted by the efficiency of the electric propulsion system as the matrices only provide the thrust power.
2. Fuel-based power checks and calculation: This part of the simulation can be found in `updateGUI.m` line 170 to line 177 for the take-off phase as an example. The simulation for cruise and landing looks similar only changing the corresponding matrices and variable names.
It checks whether enough conventional power is supplied (matrix values 2,2) to match the defined drain (matrix values 3,2, adjusted by conventional engine efficiency `turbine_eff`). If that is the case, the consumed chemical energy during the **whole flight phase** in kWh is calculated by multiplying the duration of the flight phase with the efficiency-adjusted drained power. In addition, if more chemical power is supplied than drained, the surplus of it **per time step** is computed. This surplus in chemical power is converted into electrical energy and added to the electrical energy balance. In reality this conversation could be done by a dedicated gas turbine for example. For this conversation, an efficiency factor is introduced (`eff_fuel2el` in the code) which can be set in the GUI in the "Input Variables" frame. The initial conversation efficiency is set to 0.5
If more power is drained than supplied, a boolean indicating whether the simulation is possible is set to FALSE (0 in MatLab syntax).
3. Battery checks and calculation: Starting in line 181 going to line 185 for take-off, the electrical drain is calculated. It is checked whether enough electrical power is provided to match the thrust power and electrical onboard equipment's needs. In this case, the consumed electrical energy per

time step is computed, else the sim_poss boolean is set to FALSE.

4. Do the battery energy level computation for each time step: The battery SOC is calculated for each time step, which leads to more values and a higher resolution. This higher resolution is needed because the simulation implements a battery security feature. This feature ensures that the battery does not discharge too much, as a low State of Charge (SOC) could damage it and reduce battery lifetime. The SOC relates to the percentage of available energy in the battery, in this simulation represented through a variable between 0 and 1.

It is initially set to 0.9 which means that the battery is charged 90 percent before take-off. If the battery reaches a state-of-charge smaller than 0.2 (initially, can be adjusted in the GUI in the "Main GUI" window), no more electrical power is used. In this case the electrical propulsion system is turned off but the battery is possibly charged, if a surplus in chemical power is available.

All this is done from line 193 to line 210 for take-off. The current SOC is calculated each step, compared to the threshold SOC and the battery level is updated, depending on the SOC. If the current SOC is bigger than the threshold, electric energy is drained and the battery is possibly charged. Otherwise the battery is just charged as long there is surplus in chemical energy. If no surplus is available, the energy level does not change, the electrical propulsion system is turned off in this case. The total electrical energy usage during the flight is calculated as well here.

This implementation is the reason why the total drain of chemical energy is calculated directly for the whole flight phase but all other electrical drains only for the time step. The chemical power drain is constant and its energy level does not need this high resolution whereas the battery's state-of-charge needs more sensitivity due to the threshold and the security feature.

5. Write energy levels into arrays to plot. For plotting, each calculated battery state was written into an array together with the corresponding time stamp. These arrays are plotted in the "Main GUI" window. The array contents are checked to be over zero, otherwise the sim_poss boolean goes to FALSE.

3.4 Window frames and theoretical background of shown parameters

To go on, the four different windows and their contents are presented. In the "Main GUI" and the "Metrics" window, graphical elements are used that are displayed on the active frame when a button is pressed. In order to avoid misplacement of elements like plots or LEDs in other frames, it is recommended to focus the window in use by double clicking on the grey area on the current window in use.

3.4.1 "Main GUI" window

This window is the main source of information concerning energy levels in the simulated plane. The featured plot section shows the available energy stored in batteries and fuel tanks over time of the flight and the total percentage of energy available. The x-axis represents time, the left y-axis shows energy in kWh and the right y-axis relates to the total percentage of available energy (fuel + batteries combined) compared to the beginning of flight.

To go on, the green dashed line in the plot refers to the usable energy content of the battery, the

blue line refers to the available energy stored as fuel. The orange line describes the level of total energy during flight. Colours could change if more than one instance of the simulation is opened or depending on the used operating system.

As an additional feature, two different sorts of grids can be displayed in the plot using the "Minor grid" button and "show grid" checkbox. This feature is not supported in MatLab. "Print plot" saves the shown plot as png file. The "Open plot" button opens a new window which is solely displaying the plot. "Plot battery" opens a zoomed plot into the battery state-of-charge, the battery level is plotted in green including the threshold SOC as a straight blue line. Chosen grid(s) in the main window are shown in the new plots as well. Actual simulation plots can be found in section 3.5. The simulation is started pressing "SIMULATE" while executing the simulation steps as presented above. The "Executed" LED changes its colour depending on a possible simulation with the provided input values. A green LED indicates a successful simulation, if the LED remains red, the simulation is not possible with the given values. This could be the case if more power is drained than power is provided for instance. Additionally, in this case, no plot will be shown. Whether a simulation is executable or not is checked in updateGUI.m and stored in the sim_poss boolean. A white LED is shown after the "plot graph" button is used.

If the frame does not change, this means an error occurred. This is mostly the case, if the input matrices do not describe a valid aircraft so not enough power is supplied.

The threshold box enables to set custom values for the battery's lowest state of charge which may not be undercut.

A screenshot of the "Main GUI" window after simulation can be seen in Figure 3.2.

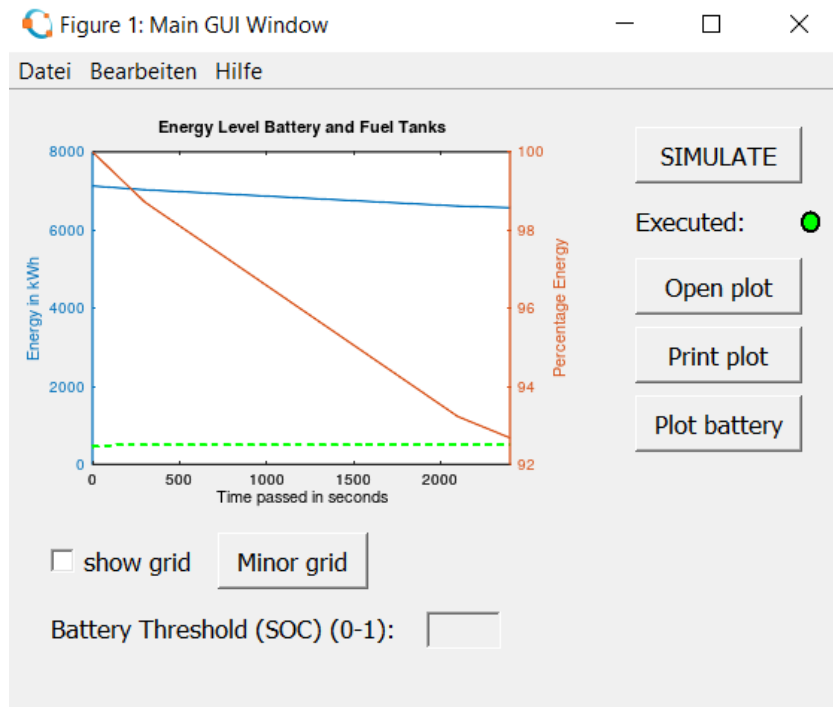


Figure 3.2: Screenshot of the "Main GUI window"

3.4.2 "Input Variables" window

The main purpose of the "Input Variables" window is to provide a convenient way to edit the values of the input matrices. Each matrix features its own section in this window. The composition of the matrix was described in the "Matrix Format" section 3.3.1.1. The abbreviation "el" implies "electrical".

In addition to the ability to edit the matrix values, some energy storage system values can be edited as well. The battery weight in kg and the capacity in kWh can be adjusted plus the state-of-charge of the battery before take-off. Moreover, the amount of loaded kerosene in kg can be specified.

The efficiency of the conventional propulsion system can be defined as well using the "CPS Efficiency" box. The conventional propulsion system (CPS) efficiency describes the conversation from chemical energy/power (stored in fuel) to actual thrust. The variable in the simulation is called "turbine_eff". The initial value for the conventional propulsion system efficiency is 0.3. This value is **not** the same as the efficiency that relates to the conversation of chemical energy to electrical energy where dedicated gas turbines optimized to generate electrical energy could be used. This variable is editable in the same window and is referred to as "Fuel2El Efficiency". The variable in the simulation is called "eff_fuel2el".

Inputs are handled through callbacks to writeInput.m from the GUI elements defined in Simulation.m. A screenshot of the "Input Variables" window after simulation can be seen in Figure 3.3.

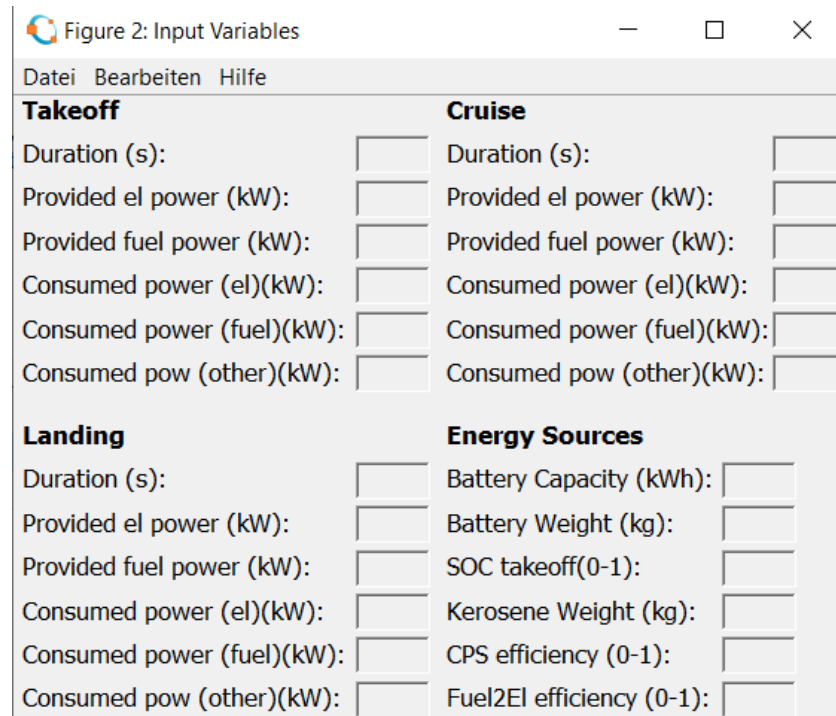


Figure 3.3: Screenshot of "Input Variables" window

3.4.3 "Insights" window

The "Insights" window supplies metrics relating to the ecological and economic impact of the mission as well as a hybrid classification of the aircraft.

The overall costs of the flight are shown, the total CO2 emissions, the degree of hybridization and the combined energy density. These metrics will be explained in the following subsections.

A screenshot of the "Insights" window after simulation with the initial values can be seen in Figure 3.4.

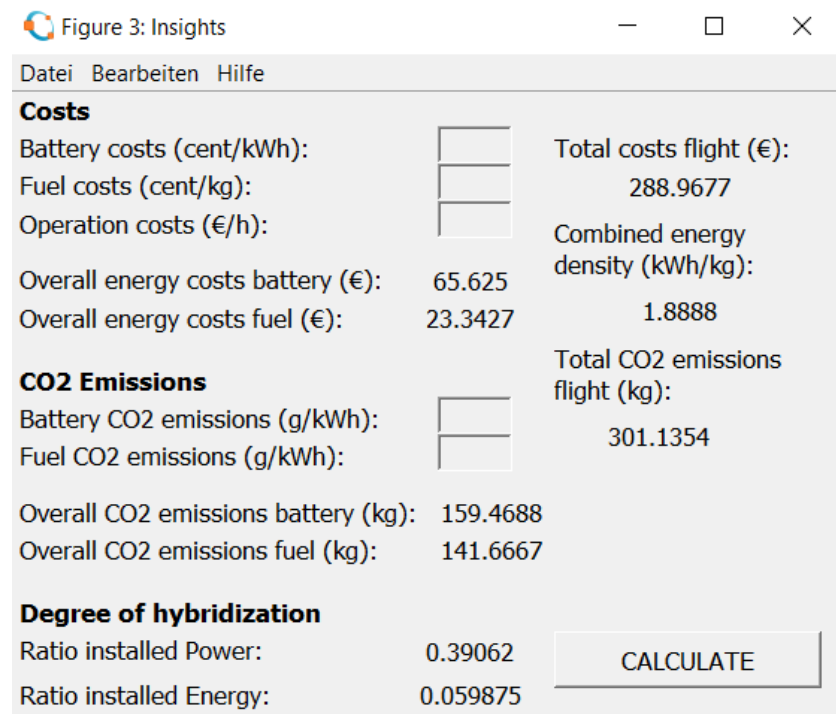


Figure 3.4: Screenshot of "Insights" window

3.4.3.1 Operating costs

Aircraft operation costs depend on many different factors like fuel prices, staff salaries or take-off and landing fees, to name a few. The "Insights" window of the simulation tool provides a simple estimation for the total operation costs of one simulated flight.

As input values, the energy costs for electrical energy and fuel are added together to all other operational costs. Operational costs are given in € per flight hour, therefore the total operational costs are calculated by multiplying them with the duration of the flight. These input values can be changed in the "Insights" window as well.

Costs for maintenance and attrition of batteries and engines could be included as well, either calculated per used amount of energy and included in the costs of the relating energy type or just in the hourly operation costs.

Energy costs are calculated in calculateMeasures.m on the basis of the energy used during flight multiplied with the energy prices.

The cost computation implementation is based on the total energy consumption. Even if the battery is charged during flight because of a surplus in chemical energy, electrical energy is drained to power the electric propulsion system. This drained energy is added up and the total is used to calculate the costs. This is the same for chemical energy.

This means that the charging of the battery does not reduce the total costs caused by the electric propulsion system as no data was available how to price one kWh generated by the conversation from chemical into electrical power.

3.4.3.2 CO₂ emissions

As presented in the state-of-the-art chapter [2], one potential of hybrid aircraft lies in the reduction of CO₂ emissions during flight. To have a quantification of CO₂ emission of one particular flight the tool calculates the emissions based on the used amount of fuel and electrical energy, similar to the calculation of the operation costs. The emitted amount of CO₂ in $\frac{g}{kWh}$ for each energy source can be adjusted in the "Insights" window. The initial value for emissions caused by the battery is 486 $\frac{g}{kWh}$ and 255 $\frac{g}{kWh}$ for fuel. All sources referring to how the initial values were chosen will be presented in detail in the "Validation and Simulation results" section [3.5].

If the battery is charged solely with renewable energy, the emissions of the electric propulsion system tend to go to zero. As a result, to have low emissions, the battery energy should be mostly renewable and its energy usage during flight should be maximized.

The presented CO₂ emissions only depict the overall mass emission of CO₂ for the whole flight. This does not take into account the environmental impact of the emissions as CO₂ during electricity production is emitted at ground level whereas CO₂ generated by burning kerosene is emitted at cruise altitude.

3.4.3.3 Degree of hybridization

To describe the energy share between the two sources in a hybrid aircraft (conventional and electrical), the degree of hybridization was introduced. It is a commonly used metric featured in many papers, in this work, the definition from [74] will be used.

The degree of hybridization is composed of two equations, one equation describing the relation of electrical energy to the total installed energy (H_E) and one equation describing the share of installed power (H_P) [74].

$$H_P = \frac{P_e}{P_{tot}} \quad (3.1)$$

$$H_E = \frac{E_b}{E_{tot}} \quad (3.2)$$

P_e describes the installed electrical power, E_b the energy content of the battery. Subscript "tot" refers to total power/energy.

In conventional aircraft, no electrical power is used to generate thrust, hence H_P and H_E are zero whereas in an all-electric aircraft H_P and H_E are both one [74]. Hybrid aircraft with both electric and fuel powered propulsors feature values for H_P and H_E between zero and one [74].

The degree of hybridization is an important measure in a hybrid aircraft and it will be used in other

calculations like range for example in the simulation tool later.

Provided power could vary during the duration of flight, as defined in the matrices. This leads to a power share that could be time dependant. To tackle this problem, the maximum values of take-off, cruise and landing of each power source are taken into account for the calculation. The maximum values for each source individually do not have to apply in the same flight phase, but the degree of hybridization is based on these maximum values. In the simulation case presented in section 3.5, the installed/provided power is constant during all flight phases.

This simplification was done in order to have clarity in the GUI while providing a best case electric power split. The implemented equation looks like this:

$$H_{P,impl} = \frac{\max(T(2,1), C(2,1), L(2,1))}{\max(T(2,1), C(2,1), L(2,1)) + \max(T(2,2), C(2,2), L(2,2))} \quad (3.3)$$

3.4.3.4 Combined energy density

As mentioned before, modern batteries possess a limited energy density compared to kerosene. It was considered as very interesting to calculate the combined energy density of the two sources in a hybrid aircraft.

The combined energy density introduced here describes the energy density of the aircraft's energy storage system if it used a single source of energy. In this thesis this relates to a combination of the energy density of the batteries and kerosene.

The calculation is very straight-forward by dividing the total energy of batteries and fuel by the total mass of both. This leads to:

$$D_{combined} = \frac{E_{batt} + E_{fuel}}{m_{batt} + m_{fuel}} \quad (3.4)$$

This information could be used to compare the performance of the plane with an alternative fuel type that features that exact energy density or give an estimation about which energy density the batteries of an all-electric aircraft would need to have in order to be able to execute the simulated flight.

In addition, the combined energy density will be used to determine the range of the hybrid aircraft.

3.4.4 "Metrics" window

Additional figures of merit are provided in the "Metrics" window, the last window featured in the GUI. The data calculated and displayed here describes the overall aircraft and its flight characteristics in a more detailed way.

On the left side of the window, boxes are placed to edit input parameters. These input values are used for various calculations of parameters in this section. On the right side the calculated constant values are displayed and buttons are featured to plot various values depending on time like weight or the required power to stay in cruise.

"Efficiency EPS" refers to the efficiency of the electric propulsion system (EPS) that is converting battery power into thrust, comparable to the conventional propulsion system efficiency.

A screenshot of the "Metrics" window after simulation with the initial values can be seen in Figure 3.5. Following, the features of the "Metrics" window are presented in detail.

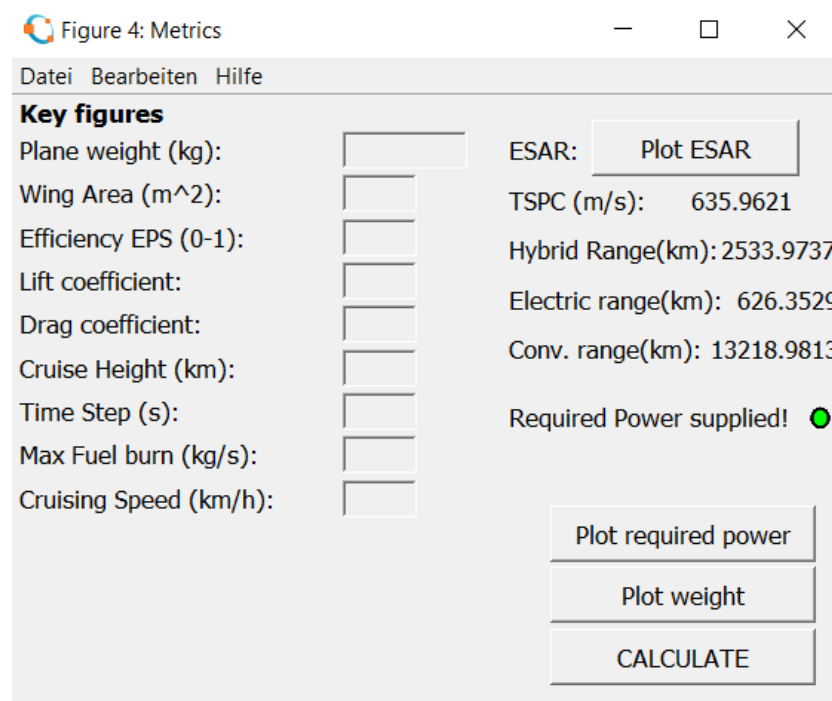


Figure 3.5: Screenshot of "Metrics" window

3.4.4.1 Required power and weight in cruise

The hybrid propulsion system uses kerosene as one source of power. As kerosene gets burnt during flight, the aircraft loses weight. Less weight leads to less required power to stay in flight as less weight force is experienced. Battery weight does not change during flight.

Pressing the "plot required power" and "plot weight" button (see Figure 3.5) will plot these parameters during cruise as the simplified physics only apply in cruise. Therefore this simulation is only implemented during cruise at the moment.

Kerosene consumed during take-off is calculated based on the drained power and already subtracted before start of the calculation of these two parameters (required power and mass loss in cruise).

To understand in depth why mass is changing in cruise, a short overview over physics of flying needs to be given. It is based on [6].

Flight physics (based on [6]) In flight an aircraft experiences four forces, lift L, drag D, thrust T and weight force W.

L is vertical to the flight path, D is parallel to the flight path directing in the opposite direction of flying. W is pointing to the centre of gravity of earth. T is facing in direction of the flight path turned by an angle σ which refers to the turning between T and the flight path. Look at Figure 3.6 for better understanding.

In a simplified model for unaccelerated horizontal flight (cruise), which is used in the simulation, drag D is compensated by thrust T and lift L compensates the weight force W. So in absolute values

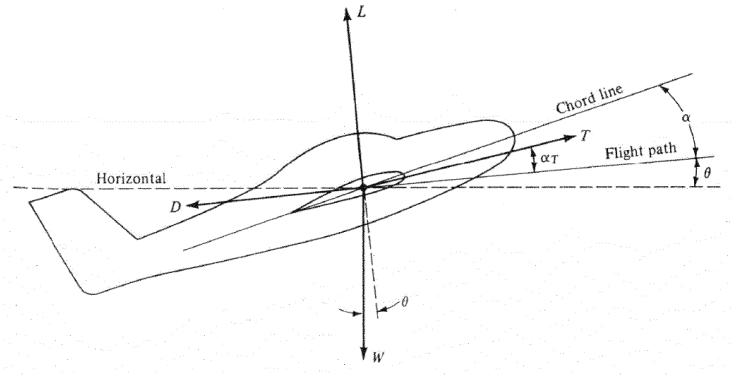


Figure 3.6: Forces in cruise, taken from [6]

these equations apply:

$$D = T \quad (3.5)$$

$$L = W \quad (3.6)$$

D is defined as

$$D = q_\infty \cdot S \cdot c_D \quad (3.7)$$

with q_∞ describing the dynamic pressure, S wing area and c_D the drag coefficient.
L is defined as:

$$L = q_\infty \cdot S \cdot c_L \quad (3.8)$$

with c_L relating to the lift coefficient. Drag and lift coefficients are expected to be constant during cruise.

By combining [3.5] [3.6] [3.7] and [3.8] an equation for thrust T can be obtained

$$T = \frac{W}{c_L/c_D} \quad (3.9)$$

The necessary driving power to stay in cruise can be obtained by

$$P_r = T \cdot V_h \quad (3.10)$$

with V_h relating to the speed in a specific height. V_h can be described by this equation

$$V_h = \sqrt{\frac{2 \cdot W}{\rho_h \cdot S \cdot c_L}} \quad (3.11)$$

with ρ_h referring to the air density at flight altitude.

Combining [3.9] [3.10] and [3.11] an equation for the required power in cruise can be obtained:

$$P_{r,h} = \sqrt{\frac{2 \cdot W^3 \cdot c_d^2}{\rho_h \cdot S \cdot c_L^3}} \quad (3.12)$$

ρ_h in the simulation is calculated based on the cruise height. For the calculations, the International Standard Atmosphere (ISA) is used including these equations to describe the temperature and pressure at cruising altitude:

$$T(h) = T_0 + \frac{dT}{dh} h \quad (3.13)$$

$$p(h) = p_0 \cdot \left(\frac{T(h)}{T_0}\right)^{5.26} \quad (3.14)$$

Together with the initial values $T_0 = 288.15 \text{ K}$ and $p_0 = 101.325 \text{ kPa}$ a final equation the pressure at cruise height can be obtained:

$$\rho_h = \frac{p(h)}{R \cdot T(h)} \quad (3.15)$$

with $R = 0.287 \frac{\text{kJ}}{\text{kg} \cdot \text{K}}$. [3.15](#) can be put in [3.12](#) to obtain the specific power at a certain height. W changes over time as the mass is changing over time. Therefore the required power needs to be recalculated after some time.

The required power calculated here is directly related to the thrust that is needed to stay in cruise. As the efficiencies of the propulsion systems are not 100 percent, this required power needs to be adjusted in further calculations by the efficiency of the propulsion system. The plot that can be shown by pressing the button in the "Metrics" frame shows the unadjusted required power for better optimization possibility.

Implementation All additionally needed input values to calculate the mass loss and required power can be entered in the "Metrics" window on the left.

The required power in cruise and mass loss are recalculated after each time step, the length of an individual step can be edited in the GUI and is initially set to 0.5 seconds. This time step defines the duration of the energy level computation presented in [Section 3.3.3](#) as well.

Before starting the actual calculation for each time step, the amount of fuel burnt during take-off is computed and used to obtain the initial starting mass at the beginning of the cruise phase.

The calculation algorithm for the required power and mass loss looks like this:

1. Calculation of the required power to stay in cruise according to [3.12](#) with current aircraft mass.
- 2.: Check if required power is bigger than the total provided power by batteries and fuel. Here, the required power is adjusted by the combined efficiency of the hybrid propulsion system described in [3.19](#) later to check whether enough power is supplied by the whole system. If not enough power is supplied, the "Required Power supplied" LED turns red. A mass loss is calculated still in this case but its significance is diminished.
3. Calculate the burnt fuel which is equal to the mass loss in one time step. To achieve this, a maximum fuel burn variable $m_{fuelburn,max}$ is introduced that describes the fuel burn of the engines at their maximum power output. The unit of this input parameter is $\frac{\text{kg}}{\text{s}}$. This variable can be set in the GUI. This fuel burn is multiplied by the fraction:

$$R_p = \frac{P_r}{P_{tot,cruise} \cdot \eta_{cps}} \quad (3.16)$$

In this implementation it was assumed that the maximum power the engines can provide (second line in the matrices) is reached in cruise. This means that the maximum fuel burn would be reached in cruise. But as probably more power is installed than actually required, the resulting fuel burn is lower as for less required power less fuel needs to be burnt. Therefore this scaling factor divides the required power by the total available power.

Nevertheless this linear model is only a simplification of an actual aircraft engine.

This relation factor R_p is multiplied with the maximum fuel burn $m_{fuelburn,max}$ and $S_c = \frac{P_{cruise,fuel}}{P_{tot}}$ to obtain the mass loss during the time step. S_c is needed to account for the two power sources in the hybrid plane as only fuel-powered engines account for the mass loss.

S_c is the power share of the conventional power in cruise. As the presented degree of hybridization above in section 3.4.3.3 does not necessarily use the matrix entries of the cruise matrix for its calculation but the maximum of all matrices, S_c was used here.

$$m_{loss,step} = R_p \cdot S_c \cdot m_{fuelburn,max} \cdot time_{step} \quad (3.17)$$

In the simulation, S_c and R_p are combined in the variable "power_av".

As fuel is only burnt by the conventional propulsion system, the required power is scaled with the efficiency of the conventional propulsion system η_{cps} in equation 3.16

4. Update aircraft mass by subtracting the burnt fuel mass from the previous aircraft mass.

The required power and the mass over time are plotted when pressing the corresponding buttons in the "Metrics" window.

It needs to be said that the mass loss is only based on the required power. The set supplied and consumed power in the C matrix are not significant for this calculation here and the calculated value is not written into C. In a future version of this tool an adaption of the consumed power could be implemented.

This being said, the model for the mass loss is not related to the energy model depicted in 3.3.3 that could also be used to calculate the mass loss. The model used and presented here is based on the plane and engine characteristics and not just on given power input values. As this model is only used in this section for this one final parameter, its significance for the total simulation is still low. To give more significance to this feature, the model including the required power needs to be transferred into the matrices as consumed power in C(2,2). As described above, this could be one main feature for a future version.

The mass loss in the other model used on the energy calculated in 3.3.3 could be acquired by using the consumed energy during cruise stored in the y_fuel array in updateGUI.m and the energy density of kerosene. This feature is not implemented yet, but was calculated for the validation case in section 3.5.2.4.

3.4.4.2 TSPC (Thrust Specific Power Consumption)

The "Thrust Specific Power Consumption" (TSPC) is introduced in [52] as a corresponding metric for electric aircraft to the "Thrust Specific Fuel Consumption" (TSFC) used in conventional aircraft. TSFC in conventional aircraft describes the ratio of fuel flow to net thrust [52].

As in hybrid applications electric propulsion is used as well to generate thrust, which does not use fuel as source of power, the TSFC is not applicable in hybrid environments. To tackle this problem, Seitz et al. introduced the TSPC measure for all-electric aircraft $TSPC_{elec}$ [52].

$TSPC_{elec}$ refers to the ratio of supplied power to net produced thrust

$$TSPC_{elec} = \frac{P_{supply}}{F_0} = \frac{V_h}{\eta_{eps}} \quad (3.18)$$

with F_0 relating to the generated thrust and η_{eps} relating to the efficiency of the electric propulsion system (from battery to thrust). The unit of TSPC is $\frac{m}{s}$

For a hybrid application this TSPC parameter needs to be adapted. In a hybrid environment, the combined efficiency of both propulsion systems needs to be used instead of only the efficiency of the electric propulsion system η_{eps} . The efficiencies are weighted by the power share, to account for the differences in installed power and therefore thrust generation. The resulting combined efficiency is:

$$\eta_{hybrid} = (H_P \cdot \eta_{eps}) + (1 - H_P) \cdot \eta_{cps} \quad (3.19)$$

with η_{cps} describing the efficiency chain of the conventional propulsion system. In the simulation tool η_{cps} is called "turbine_eff" (initially set to 0.3) and η_{eps} is called "eps_effi" (initially set to 0.8). η_{hybrid} is assumed to be constant during flight.

The final TSPC parameter for hybrid aircraft using the initial definition [3.18] is:

$$TSPC_{hybrid} = \frac{P_{supply}}{F_0} = \frac{V_h}{\eta_{hybrid}} \quad (3.20)$$

3.4.4.3 ESAR (Energy Specific Air Range)

Seitz et al. state in [52] that metrics based purely on the efficiency of the propulsion system are insufficient for describing aircraft performance. Therefore a figure of merit at aircraft level is required, which is independent from the source of energy [52]. The often-used Specific Air Range (SAR) in conventional aircraft was taken and extended to be applicable in a hybrid environment. This extended parameter is called "Energy Specific Air Range" [52].

It is defined in equation [3.21] and its unit is $\frac{1}{N}$.

$$ESAR = \frac{dR}{dE} = \frac{V_h \cdot c_L/c_D}{TSPC \cdot m_{plane} \cdot g} = \frac{\eta_{hybrid} \cdot c_L/c_D}{m_{plane} \cdot g} \quad (3.21)$$

ESAR or $\frac{dR}{dE}$ describes the change of aircraft range per change of energy [52]. As the mass is changing throughout the cruise phase, ESAR is time-dependant as well [52]. The other components of the equation are assumed to be constant as an approximation to reality. In reality, parameters like the lift and drag coefficients c_D and c_L are not constant during flight [52]. Hence a button was implemented in the GUI that plots ESAR over time.

3.4.4.4 Ranges

Range may be the most important performance factor of an aircraft besides costs. Therefore estimation equations for range were implemented and the results are shown in the "Metrics" window. Featured there are the hybrid range, the electric range of the same aircraft (so no fuel is loaded) and the conventional range (same aircraft without batteries). The presented range equations are based on the well-known Breguet range equation. In all equations, g was expected to be $9.81 \frac{m}{s^2}$ as a constant value.

Electric range The implementation of the electric range was seen as mean to determine the performance of the hybrid range in comparison to an all-electric version.

Voskuyl et al described the range for an all-electric plane in their work [75], their definition will be used in this thesis. In all-electric planes H_P and H_E are both one (as presented previously) and the equation results in:

$$R_{electric} = \eta_{prop} \cdot \eta_{eps} \cdot \frac{c_L}{c_D} \cdot \frac{D_{bat}}{g} \cdot \frac{m_{bat}}{m_{bat} + m_{plane}} \quad (3.22)$$

η_{prop} describes the efficiency of the propeller and was assumed to be 1 for all ranges, as all efficiencies of the propulsion systems are included in the η_{eps} and η_{cps} efficiencies. D_{bat} refers to the energy density of the battery in $\frac{J}{kg}$

Conventional range For conventional aircraft, H_P and H_E are both 0, the resulting equation was presented as following in [76]:

$$R_{conventional} = \eta_{cps} \cdot \frac{c_L}{c_D} \cdot \frac{D_{fuel}}{g} \cdot \ln\left(\frac{m_{plane} + m_{fuel}}{m_{plane}}\right) \quad (3.23)$$

D_{fuel} refers to the energy density of fuel in $\frac{J}{kg}$ which is 42840000 $\frac{J}{kg}$ for kerosene (11.9 $\frac{kWh}{kg}$) [28].

Hybrid range In literature many equations for hybrid flying can be found. Unfortunately they are often based on very unconventional parameters, therefore it was decided to adapt the equation for conventional range by using the combined energy density and combined propulsion system efficiency presented previously. The equation adapts the equation for conventional range, but changes the logarithmic part as well as the the efficiency and the energy density. The resulting equation looks as following:

$$R_{hybrid} = \eta_{hybrid} \cdot \frac{c_L}{c_D} \cdot \frac{D_{combined}}{g} \cdot \ln\left(\frac{m_{plane} + m_{fuel} + m_{batt}}{m_{plane} + m_{batt}}\right) \quad (3.24)$$

$D_{combined}$ relates to the combined energy density presented above in $\frac{J}{kg}$ and therefore needs to be converted in the tool before calculation. The logarithmic part of the equation was designed according to the hybrid range equation presented in [75].

Implementation The implementation of the equations is quite straight forward, some repeating parts were assigned to their own variables for better re-usability and easier readability. Code starts at line 155 in calculateMetrics.m

The range of an aircraft is dependent on the amount of energy that is available for flying. In conventional aircraft fuel is burned to provide energy and the plane loses mass during flight, in all-electric aircraft only batteries supply energy and the plane does not loose mass in flight. This effect causes differences in the equations.

A more detailed discussion of results will be given in the next section.

3.5 Validation and simulation results

In this last section of the simulation chapter, the validation data that was used to test and validate the tool will be presented as well as the simulation results for it. The validation data also serves as

initial values for the simulation.

The validation data was chosen to depict a 19-seater aircraft similar to the concept plane presented in [17].

3.5.1 Validation data

3.5.1.1 Mass breakdown

The mass of the simulation plane is based on the E-19 concept plane described in [17]. To stay in the same certification envelope CS23 for commuter planes, MTOW was set to 8618 kg as done in [17] to ensure commuter plane certifications (CS23). This maximum weight is composed of the battery weight, plane weight and maximum loadable fuel weight.

m_{plane}	4603 kg
m_{bat}	2018 kg
m_{fuel}	1997 kg

Table 3.1: Mass breakdown of simulated plane based on [17]

3.5.1.2 Propulsion systems parameters

In this section parameters of the electric propulsion and conventional propulsion system are presented.

Electric propulsion system With the given values energy density of the battery yields 250 Wh/kg. As discussed in the state-of-the-art chapter, this density is ambitious with modern battery system, but not unrealistic.

Initial SOC	0.9
SOC threshold	0.2
EPS Efficiency	0.8
m_{bat}	2018 kg
Battery capacity	504.5 kWh

Table 3.2: Data of the simulated electric propulsion system

Conventional propulsion system The maximum fuel burn is based on the data of a Dornier 228 Advanced Commuter aircraft with 19 seats and fuel burn of $0.945 \frac{kg}{km}$ [77]. This fuel burn is multiplied with the average cruise speed of $315 \frac{km}{h}$, which will be presented in the "Aerodynamic parameters" section 3.5.1.4 of this chapter. Dividing the result by 3600 results in a fuel burn of $0.083 \frac{kg}{s}$.

Gas turbines for power generation tend to have an efficiency between 50 and 30 % [78]. In combination with efficiencies for all other systems (propellers, fuel pumps, etc) the overall efficiency of the conventional propulsion system was estimated to be 0.3.

m_{fuel}	1997 kg
Max fuel burn	0.083 kg/s
CPS Efficiency	0.3

Table 3.3: Data of the simulated conventional propulsion system

3.5.1.3 Costs and emissions

CO2 intensity for electricity in Germany for 2017 is stated by Paul et al to be $486 \frac{g}{kWh}$ [18]. To obtain one kWh by burning kerosene, between 250 and 260 grams of CO2 are emitted, depending on the sort of kerosene [79][80]. The mean average of both sources is used for the simulation, resulting in $255 \frac{g}{kWh}$.

Household prices for electricity in Germany were around 25 to 30 cents/kWh during the last decade with current prices for one kWh of 28.73 cents [81]. As these are household prices and commercial prices are assumed to be lower, 20 cents/kWh are used in the simulation.

Kerosene prices depend on the global oil price which was declining during the Corona crisis. Kerosene prices were around 0.6 \$ per gallon [82], but based on older data from 2019 the price of energy yielded by kerosene is set to 50 cents/kWh in the simulation.

Operational costs per hour are estimated to be 300 €, based on [20]. These cover all costs including attrition.

CO2 emissions electricity	$486 \frac{g}{kWh}$
Co2 emissions fuel	$255 \frac{g}{kWh}$
energy costs electricity	$20 \frac{\text{cent}}{kWh}$
energy costs kerosene	$50 \frac{\text{cent}}{kWh}$
Operational costs per hour	300 €

Table 3.4: Cost and emission data

3.5.1.4 Aerodynamic parameters

These parameters are mainly used in calculations shown in the "Insights" and "Metrics" windows of the GUI. These input parameters include wing area, lift and drag coefficients or cruise height.

Wing area was adopted from the E-19 plane [17] as well as cruise speed which is estimated in the simulation with 315 km/h (170 knots) [17]. The initial lift coefficient used in the simulation is based on [83] and the drag coefficient is based on [84]. These initial values are highly depending on the aircraft's geometry and should be seen more as a starting point.

Cruise height is given in [17] with a minimum altitude of 10000 ft up to 25000 ft maximum cruise height. As a reference, a cruise height of 23000 ft (7000 m) was chosen. This cruise height relates to an air density of $0.5895 \frac{kg}{m^3}$. In the current version of the tool, only the air density can be entered relating to cruise height as initial parameter in the code. An input box for entering the cruise height can be found in the "Metrics" window of the GUI.

Wing area [17]	33.2 m ²
Lift coefficient [83]	1.4
Drag coefficient [84]	0.05
Cruise height [17]	23000 ft
Cruise speed [17]	315 km/h

Table 3.5: Aerodynamic data

3.5.1.5 Flight matrices

The simulated flight was designed with a total flight time of 40 minutes, 30 minutes in cruise and both 5 minutes in take-off and landing. The supplied power by battery and kerosene remains constant in all flight phases.

To determine the flight matrices, the Do228 from before is used and previous simulation results. The Do228 uses two TPE331-10 engines that provide a maximum power of 700 kW each [77] [85]. From previous simulations it is known that the required power to stay in cruise (unadjusted) is between 200 kW and 300 kW. As a result, 250 kW were taken as basis for the unadjusted required power. The adjusted power results in 833.33 kW adjusted by the efficiency of the conventional propulsion system. The following matrices are based on this estimation.

During take-off, all power provided by both sources is needed, 525 kW are used in the electric propulsion system as thrust, 350 kW in the conventional propulsion system and 75 kW for all other electric equipment onboard.

In cruise, it was assumed that the drain of thrust power caused by the electric propulsion system is 300 kW, 250 kW for conventional propulsion and 100 kW for all other onboard electrical equipment. This can be explained by meal servings and other amenity equipment. The power consumption by all other onboard electrical equipment is based on the assumptions and calculations presented in section 2.2.4.6 the other assumptions on required power values from previous simulations as presented above.

In landing, drained power is lowered to 100 kW electrical propulsion, 150 kW in conventional propulsion and 50 kW for electrical onboard equipment.

The resulting matrices look like this:

$$T = \begin{pmatrix} 300 & 0 & 0 \\ 750 & 1170 & 0 \\ 525 & 350 & 75 \end{pmatrix} C = \begin{pmatrix} 1800 & 0 & 0 \\ 750 & 1170 & 0 \\ 300 & 250 & 100 \end{pmatrix} L = \begin{pmatrix} 300 & 0 & 0 \\ 750 & 1170 & 0 \\ 100 & 150 & 50 \end{pmatrix}$$

It needs to be stated

again that the power stored in the third line of the matrices is only relating to the actual thrust. To obtain the total drain from the onboard power distribution system, the drained powers need to be adjusted by the corresponding efficiency.

3.5.2 Simulation results

With the given initial values, interesting simulation results can be obtained. Results were rounded to two decimal places in most cases. Firstly, only results are presented, following in the "Discussion and analysis" section 3.5.3 these results are discussed.

3.5.2.1 Main simulation

It can be seen that a simulation with the provided values is perfectly possible as all LEDs turn green.

During take-off the battery is slowly charged until its maximum capacity is reached. During all other flight phases enough power is provided by fuel to power both the conventional and electrical propulsion system, so no more battery energy is drained.

The level of fuel is lowered in all flight phases. The plots can be found in Figures 3.7 and 3.8.

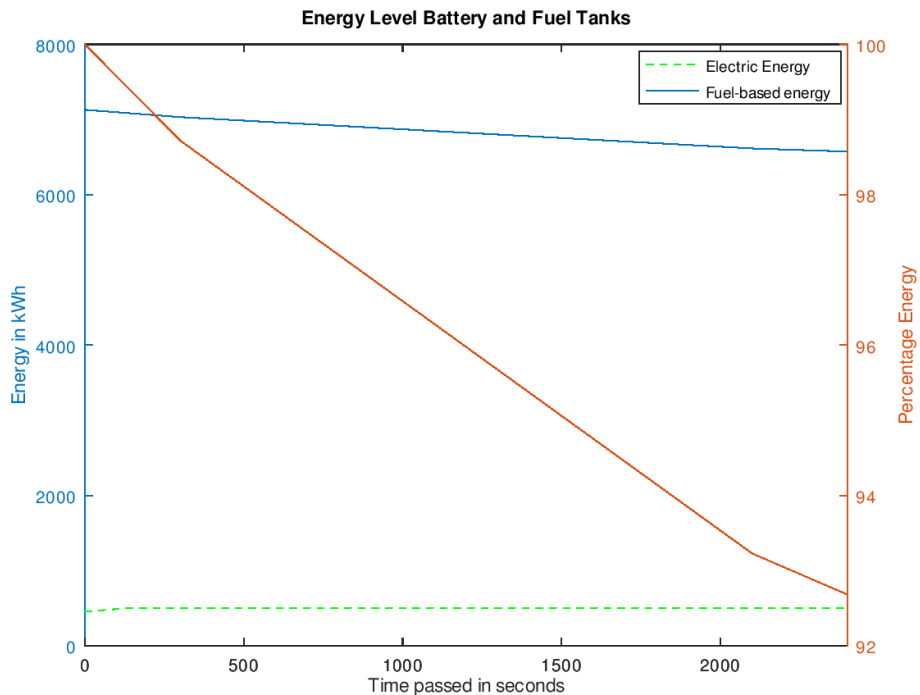


Figure 3.7: Energy levels during flight

3.5.2.2 Costs and emissions

The total energy costs of battery energy are 65.63 € and 23.34 € in total fuel costs. The total flight costs aggregate then to 288.97 € for this 40 minutes flight including operation costs.

In total 301.14 kg of CO₂ were emitted during this flight, 159.47 kg by the energy of the battery and 141.67 by burning fuel. These values can also be seen in figure 3.4.

3.5.2.3 Degree of hybridization and combined energy density

With equation 3.4 presented above, the combined energy density of the plane results in 1.89 $\frac{kWh}{kg}$. This energy density is only 15.9 % of the energy density of kerosene, but 7.56 times the energy

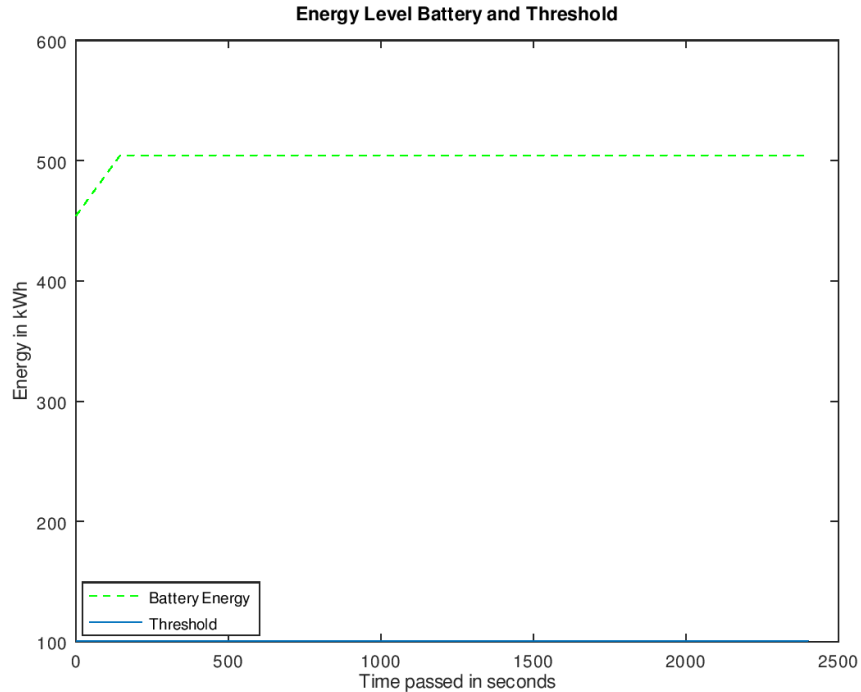


Figure 3.8: Zoom into battery state of charge

density of the battery system.

H_P is calculated to be 0.39, which means that 39 % of total installed power are electric power. H_E results in 0.06 which indicates that roughly 6 % of total installed energy are electrical energy. These values can also be seen in Figure 3.4

3.5.2.4 Required power and mass loss

Required power during cruise at beginning is 236.1 kW and drops linearly to 234.53 kW in the end. This results in a percental loss of 0.66 percent compared to the start of cruise. It can be easily seen that more power is provided than power is needed to stay in cruise.

Plane mass in this model starts at 8590.6 kg and drops to 8553.7 kg at the end of cruise, resulting in a fuel burn of 36.9 kg during cruise. This is a percental loss of 0.43 percent compared to the start of the cruise phase. This model will be called the "power model" in some parts of the discussion part later. This is the experimental mass loss described in 3.17 calculated for the whole cruise phase.

The mass loss was also calculated based on another model to evaluate the performance of the model presented above. This second model will be referred to as the "energy model". In this second model, the actual consumed energy was taken and divided by the energy density of kerosene.

The energy level of the fuel tanks is stored in the `y_fuel` array in the simulation code in `updateGUI.m`. To calculate the energy consumed in cruise, the second value (relating to the energy level after

take-off) is taken and the third value (relating to the energy level after the cruise phase) is subtracted from it. As a result, 416.7 kWh are consumed by the conventional propulsion system during cruise. This energy is already adjusted by the efficiency of the conventional propulsion system. To obtain the final amount of burnt fuel, 416.7 kWh are divided by $11.9 \frac{kWh}{kg}$, the energy density of kerosene. This results in a mass loss of 35.0 kg.

This is a very interesting result, the analysis of these results will be given in the [3.5.3](#) section.

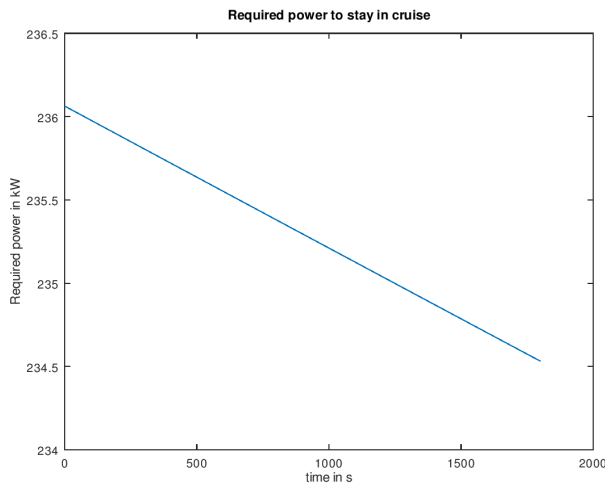


Figure 3.9: Power during cruise

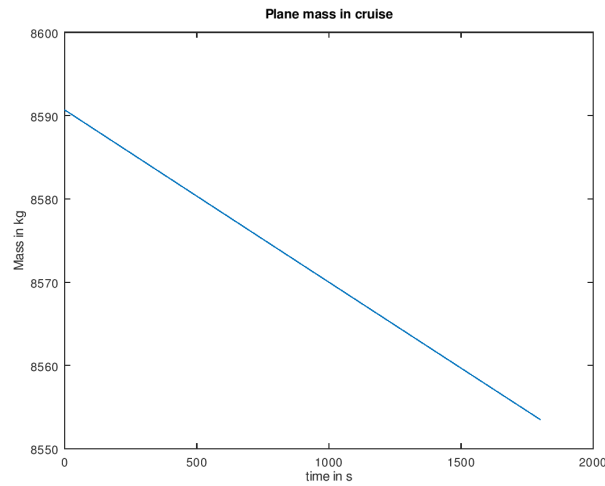


Figure 3.10: Mass of plane during cruise

3.5.2.5 ESAR and TSPC

With the provided initial values TSPC results in $635.96 \frac{m}{s}$. ESAR is time-dependent and rises during cruise, starting at $0.1645 \cdot 10^{-3} \text{ 1/N}$ going up to $0.1653 \cdot 10^{-3} \text{ 1/N}$. These values can also be seen in Figure 3.5

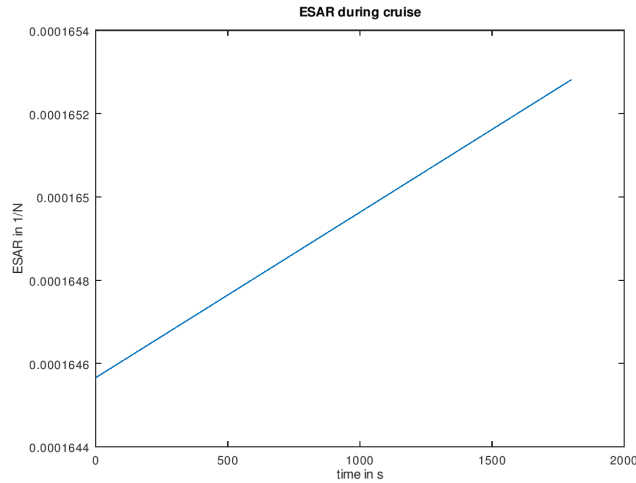


Figure 3.11: ESAR during cruise

3.5.2.6 Ranges

Ranges are one of the most important parameters in aircraft design. With the presented initial parameters the electrical range of the plane is 626.35 km, the conventional range 13218.98 km and its hybrid range results in 2533.97 km. These values can also be seen in Figure 3.5

3.5.3 Discussion and analysis

It can be seen that during this test flight only around 5 % of total energy is used. This indicates that the validation data is very optimistic as 19-seater usually do not fly long routes [18]. Less kerosene could be loaded in order to reduce weight and emissions.

If you look at Figure 3.8 it can be seen that the battery is recharged fast during take-off. This implies that less chemical power or more electrical power could be installed to have an optimal result.

It can be seen that the drop in required power and total aircraft mass are probably quite insignificant in this scenario with losses under 0.5 %. The changes in ESAR are also quite insignificant. Therefore ESAR could be seen as a constant in this simulation example. The mean average of ESAR could be shown as a constant in a future version of the tool instead.

The comparison of the two models describing the mass loss (the "energy model" and the "power model") is interesting. Both results are in the same range, with 35.0 kg (energy model) and 36.9 kg

(power model). This shows that the models perform equally good in this particular simulation case. Nevertheless a fuel burn of 36.9 kg maximum seems to be quite ambitious for a hybrid plane during 30 minutes of cruise. The Do-228, used previously for the estimation of the fuel burn per second, has a hourly fuel burn of around $200 \frac{kg}{h}$ [86][87], resulting in around 100 kg for the cruise phase in the simulation setting with a conventional aircraft. As the simulated plane has a power hybridization factor of 0.39, 61 percent of the installed power are conventionally generated by fuel. This would result in a fuel burn of 61 kg during cruise, still much higher than the fuel burns calculated by the models.

In the power model, the required power is divided by the hybrid efficiency η_{hybrid} and weighted to the total installed power (and later multiplied with the degree of hybridization of conventional power). This fraction results in $\frac{235}{(300+250)}$, which is 0.43 (as both parts of the fraction would need to be multiplied with η_{hybrid} , it gets cancelled out). This means that much more power is installed than needed and as the model scales the fuel consumption linearly by this fraction, it results in this quite low fuel burn in the model.

To conclude, the results of the models seem to low to match the actual fuel burn in this example. The reason for this could be that the input matrices are chosen inappropriately or the models are not describing the aircraft's characteristics in a good manner. The input matrices were not only chosen to match a real aircraft but also to show the features of the simulation.

The most interesting results can be found among the ranges. It might seem intuitive that the hybrid range is the sum of the electrical and the conventional range, but this is not the case.

The logarithmic part of the equations [3.24] and [3.23] are not the same as in the hybrid range the battery weight needs to be taken into account. Nevertheless they do not differ that much in number in this example, the logarithmic part for the conventional range results in 0.36036, for the hybrid range it results in 0.26361. Therefore the hybrid logarithmic factor is about 72 % of the conventional factor.

The real reason why the hybrid range differs that much from the conventional range can be found in the combined energy density.

The differences in the energy densities in both energy types are significant, kerosene with $11.9 \frac{kWh}{kg}$ and the battery density with $0.25 \frac{kWh}{kg}$, which is a difference of around two magnitudes. Of course much more chemical power is installed but this can only partly compensate the small energy density of the batteries. This results in an overall combined energy density of $1.89 \frac{kWh}{kg}$, roughly 10 % of the energy density of kerosene.

Both the smaller logarithmic factor and the combined energy density can only be partly compensated by the higher combined efficiency η_{hybrid} (48.75 %) which is 20 percentage points higher than the efficiency of the conventional propulsion system.

Combining all these arguments, the resulting hybrid range of 2492.01 km seems quite impressive and to be a good estimation. Nevertheless the resulting hybrid and conventional ranges are really high in comparison to the state-of-the-art aircraft. The range is not unrealistic but seems very ambitious. In modern aircraft these ranges barely will be achieved.

With the help of this data and the provided software tool it is possible to get an estimation of the most important parameters of the hybrid propulsion system. These include range, cost, emissions and the degree of hybridization. These parameters can be used to optimize the propulsion system of the aircraft to tackle the formulated problems in [1.1]

Chapter 4

Conclusion and outlook

The presented simulation tool can be seen more as a basic framework. In the future, the tool could be enhanced and options could be added like adaption of the matrices based on the required cruise power. Time dependant entries could be allowed as inputs in the matrices, or an arbitrary number of flight phases could be thinkable to have higher simulation resolution. This would require the support of more than 3 power input matrices. More insights could be added or a matrix format for the input parameters for the simulated plane could be developed to make transfers between different tools easier.

Required power in this version only applies during cruise. This could be enlarged for all flight phases. Moreover, advanced cost calculation could be added, including negative costs for charging the battery with the spare chemical energy.

The final goal of the tool could be to calculate the optimum of all relevant parameters of the propulsion system based on input data like weight, range requirements and costs and adapt the input parameters if necessary.

Needless to say, a lot of work needs to be done to have this desired complete simulation of the hybrid environment of a hybrid aircraft.

As a conclusion it should be mentioned that hybrid flying provides many opportunities and big potentials in the future aviation market. Current hybrid aircraft technology is still very new. Fortunately, research has intensified in the last decade and advancements can already be seen as big companies try to push hybrid technology even further.

Nevertheless the biggest problem of hybrid technology is the limited battery capacity and this will also be true at least for the next 20 years. Even if the energy density of batteries advances to $1 \frac{kWh}{kg}$, as stated as possible in section 2.2.3 this is only around 10 percent of the energy density of kerosene [28].

As weight is the most significant factor in aviation, energy-dense power sources are needed which would contradict the use of current battery-technology in aerial applications.

But battery technology is advancing rapidly, also driven by companies like Tesla aiming to satisfy the demand for electric cars with extended ranges. These advancements in battery technology could possibly be boosting hybrid aviation and make short haul flights with hybrid aircraft possible in the next 20 to 30 years. An entering of hybrid planes at a wider scale would reveal potentials like reduced CO₂ emissions, shorter travel times or more freedom in aircraft design like distributed

propulsion systems.

If the presented (all-electric) concept planes like the Eviation Alice are a success and keep their promised technical specs, they could be a prototype for future hybrid commercial applications and give an preview how a hybridized aviation industry could look like.

Bibliography

- [1] H. Zhang, C. Saudemont, B. Robyns, and M. Petit. Comparison of technical features between a more electric aircraft and a hybrid electric vehicle. In *2008 IEEE Vehicle Power and Propulsion Conference*, pages 1–6, 2008.
- [2] Matti Blume. Alice picture. <https://www.chemie.de/lexikon/Kerosin.html> 2020. [Online accessed 11.05.2020].
- [3] Monroe Conner. Nasa armstrong fact sheet: Nasa x-57 maxwell. <https://www.nasa.gov/centers/armstrong/news/FactSheets/FS-109.html> 2018. [Online accessed 21.04.2020].
- [4] Accel picture. <https://www.flickr.com/photos/rolls-royceplc/49241890676/in/photostream/> 2020. [Online accessed 11.05.2020].
- [5] Ampaire official press website. <https://www.ampaire.com/news/press-release-general-aviation-pilots-071719> 2020. [Online accessed 04.05.2020].
- [6] Flugmechanik. https://tu-dresden.de/ing/maschinenwesen/ilr/ressourcen/dateien/tfd/studium/dateien/Flugmechanik_V.pdf?lang=de 2020. [Online accessed 17.06.2020].
- [7] Frank Anton. aircraft: Hybrid-elektrische antriebe für luftfahrzeuge. https://www.bbbaa.de/fileadmin/user_upload/02-preis/02-02-preistraeger/newsletter-2019/02-2019-09/02_Siemens_Anton.pdf 2019. [Online accessed 21.04.2020].
- [8] Julia Hetz Thierry Olbrechts Frank Anton, Olaf Otto. Disrupting the way you will fly! <https://www.ie-net.be/sites/default/files/Siemens%20eAircraft%20-%20Disrupting%20Aircraft%20Propulsion%20-%202000%20JH%20TH0%20-%2020180427.cleaned.pdf> 2018. [Online accessed 21.04.2020].
- [9] Magnix products site. <https://magnix.aero/products/> 2020. [Online accessed 22.04.2020].
- [10] Arrano data sheet. <https://www.easa.europa.eu/sites/default/files/dfu/TCDS%20ARRANO%201%20Initial%20Issue.pdf> 2020. [Online accessed 24.04.2020].
- [11] Ardiden data sheet. https://www.easa.europa.eu/sites/default/files/dfu/TCDS%20E103_issue%2002.pdf 2020. [Online accessed 24.04.2020].
- [12] Mtr390 data sheet. <https://www.mtr390.com/product/technical-information> 2020. [Online accessed 24.04.2020].

- [13] Cts800-4n data sheet. https://www.easa.europa.eu/sites/default/files/dfu/EASA-TCDS-E.232_%28IM%29_Light_Helicopter_Turbine_Engine_Company_%28LHTEC%29_series_engines-01-04082008.pdf, 2020. [Online accessed 24.04.2020].
- [14] Ae2100 data sheet. https://web.archive.org/web/20131228074438/http://www.rolls-royce.com/Images/AE2100_tcm92-6712.pdf, 2020. [Online accessed 24.04.2020].
- [15] Kokam aviation batteries brochure. http://m.kokam.com/data/filebox/Kokam_UAV_Brochure_0.8.pdf, 2020. [Online accessed 02.05.2020].
- [16] Borgwarner hermes technical data. https://cdn.borgwarner.com/docs/default-source/default-document-library/battery-module-product-sheet.pdf?sfvrsn=acdd823c_6, 2020. [Online accessed 02.05.2020].
- [17] Fabian Peter Thomas Zill Georgi Atanasov, Jasper van Wensveen. Electric commuter transport concept enabled by combustion engine range extender. 2019.
- [18] G. Atanasov J. van Wensveen F. Peter A. Paul, W. Grimme. Evaluation of the market potential and technical requirements for thin-haul air transport. 2019.
- [19] David Lee, David Fahey, Piers Forster, Peter Newton, Ron Wit, Ling Lim, Bethan Owen, and Robert Sausen. Aviation and global climate change in the 21st century. *Atmospheric Environment*, 43:3520–3537, 07 2009.
- [20] Eavia aircraft: Bereits 92 elektro-flugzeuge aus israel verkauft. <https://www.heise.de/newsticker/meldung/92-Elektro-Flugzeuge-aus-Israel-geordert-4499068.html>, 2019. [Online accessed 27.04.2020].
- [21] E-fan. <https://www.tagesspiegel.de/gesellschaft/panorama/kleiner-elektroflieger-kommt-airbus-zuvor-e-flugzeuge-ueberqueren-aermelkanal/12040938.html>, 2020. [Online accessed 01.07.2020].
- [22] Alice data sheet. <https://www.eviation.co/aircraft/>, 2020. [Online accessed 27.04.2020].
- [23] Clément Pernet. Electric drives for propulsion system of transport aircraft. In Miroslav Chomat, editor, *New Applications of Electric Drives*, chapter 5. IntechOpen, Rijeka, 2015.
- [24] Askin Isikveren, Arne Seitz, Patrick Vratny, Clément Pernet, and Kay Plötner. Conceptual studies of universally-electric systems architectures suitable for transport aircraft. 09 2012.
- [25] Holger Kuhn, Arne Seitz, L Lorenz, Askin Isikveren, A Sizmann, and Bauhaus Luftfahrt. Progress and perspectives of electric air transport. 09 2012.
- [26] Daniel Schlabe and Jens Lienig. Energy management of aircraft electrical systems - state of the art and further directions. 10 2012.
- [27] Oliver Schmitz and Mirko Hornung. Unified applicable propulsion system performance metrics. volume 135, 06 2013.
- [28] Kerosene data. <https://www.chemie.de/lexikon/Kerosin.html>, 2020. [Online accessed 11.05.2020].

- [29] Patrick Vratny, Corin Gologan, Clément Pernet, Askin Isikveren, and Mirko Hornung. Battery pack modeling methods for universally-electric aircraft. 09 2013.
- [30] Siemens press release. Siemens sells electric aircraft-propulsion business to rolls-royce. <https://press.siemens.com/global/en/pressrelease/siemens-sells-electric-aircraft-propulsion-business-rolls-royce> 2019. [Online accessed 20.04.2020].
- [31] E-fan x: the hybrid-electric commercial airliner. <https://www.rolls-royce.com/innovation/propulsion/regional-aircraft.aspx> 2020. [Online accessed 21.04.2020].
- [32] Grazia Vittadini. Our decarbonisation journey continues: looking beyond e-fan x. <https://www.airbus.com/newsroom/stories/our-decarbonisation-journey-continues.html>, 2020. [Online accessed 27.04.2020].
- [33] Volker K. Thomalla. Siemens-elektromotoren treiben die eviation alice an. <https://www.aerobuzz.de/general-aviation/siemens-elektromotoren-treiben-die-eviation-alice-an/> 2019. [Online accessed 21.04.2020].
- [34] Emrax website. <https://emrax.com/> 2020. [Online accessed 21.04.2020].
- [35] Emrax-188 data sheet. https://emrax.com/wp-content/uploads/2020/03/emrax_188_technical_data_table_graphs_5.4.pdf 2020. [Online accessed 21.04.2020].
- [36] Emrax-208 data sheet. https://emrax.com/wp-content/uploads/2020/03/emrax_208_technical_data_table_graphs_5.4.pdf 2020. [Online accessed 21.04.2020].
- [37] Emrax-228 data sheet. https://emrax.com/wp-content/uploads/2020/03/emrax_228_technical_data_table_graphs_5.4.pdf 2020. [Online accessed 21.04.2020].
- [38] Emrax-268 data sheet. https://emrax.com/wp-content/uploads/2020/03/emrax_268_technical_data_table_graphs_5.4.pdf 2020. [Online accessed 21.04.2020].
- [39] Emrax-348 data sheet. https://emrax.com/wp-content/uploads/2020/03/emrax_348_technical_data_table_graphs_5.4.pdf 2020. [Online accessed 21.04.2020].
- [40] Magnix website. <https://magnix.aero/>, 2020. [Online accessed 22.04.2020].
- [41] Turboshaft engine. https://www.skybrary.aero/index.php/Turboshaft_Engine 2020. [Online accessed 22.04.2020].
- [42] Eray Dincer Jonas Felix Lambert Eichler Thomas Ferguson Humza Mirza Miguel Nu-no Miguel Yael Pereda* Martin Valley Jason Bonni, Bianca Burghoff. Conceptual design of a low noise hybrid passenger aircraft. 2017.
- [43] Jonathan Stober Felix Ladwein Florian Will Jonas Mangold, Michael Lang. Hybird aircraft concept. 2019.
- [44] E-fan x power grid concept. <https://press.siemens.com/global/de/feature/grossprojekt-zur-elektrifizierung-der-luftfahrt> 2020. [Online accessed 04.05.2020].

- [45] Safran website. <https://www.safran-group.com/group-0#3>, 2020. [Online accessed 24.04.2020].
- [46] Alan Boyle. Zunum aero picks safran to build engine turbines for future hybrid electric aircraft. <https://www.geekwire.com/2018/zunum-aero-picks-safran-build-engine-turbines-next-gen-hybrid-electric-aircraft/>, 2020. [Online accessed 24.04.2020].
- [47] T700-401c data sheet. <https://www.geaviation.com/sites/default/files/datasheet-T700-401C-701C.pdf>, 2020. [Online accessed 24.04.2020].
- [48] T700-701d data sheet. <https://www.geaviation.com/sites/default/files/datasheet-T700-701D.pdf>, 2020. [Online accessed 24.04.2020].
- [49] T700-701k data sheet. <https://www.geaviation.com/sites/default/files/datasheet-T700-701K.pdf>, 2020. [Online accessed 24.04.2020].
- [50] T700/t6a1 data sheet. <https://www.geaviation.com/sites/default/files/datasheet-T700-T6A.pdf>, 2020. [Online accessed 24.04.2020].
- [51] Cts800 product website. <https://www.rolls-royce.com/products-and-services/defence/aerospace/rotary/cts800.aspx#/>, 2020. [Online accessed 24.04.2020].
- [52] Arne Seitz, Oliver Schmitz, Askin Isikveren, and Mirko Hornung. Electrically powered propulsion: Comparison and contrast to gas turbines. 09 2012.
- [53] Julian Hoelzen, Yaolong Liu, Boris Bensmann, Christopher Winnefeld, Ali Elham, Jens Friedrichs, and Richard Hanke-Rauschenbach. Conceptual design of operation strategies for hybrid electric aircraft. *Energies*, 11:217, 01 2018.
- [54] Documentation working conditions for rare earth element miners. <https://www.ezef.de/publikationen/sklavenarbeit-fuer-unseren-fortschritt/2949>, 2020. [Online accessed 14.07.2020].
- [55] Environmental damages due to lithium mining. https://www.deutschlandfunk.de/lithium-abbau-in-suedamerika-kehrseite-der-energiewende.724.de.html?dram:article_id=447604, 2020. [Online accessed 14.07.2020].
- [56] Kokam history. <http://kokam.com/about-us/>, 2020. [Online accessed 02.05.2020].
- [57] Kokam cell specification. <http://kokam.com/cell/>, 2020. [Online accessed 02.05.2020].
- [58] Borgwarner website. <https://www.borgwarner.com/home>, 2020. [Online accessed 02.05.2020].
- [59] Tesla model s battery data. https://www.nasa.gov/sites/default/files/atoms/files/17_-_tesla_-_success_story_or_hype_ver_3_deleon.pdf, 2020. [Online accessed 02.05.2020].
- [60] Panasonic starts mass-production of high-capacity 3.1 ah lithium-ion battery. <https://news.panasonic.com/global/press/data/en091218-2/en091218-2.html>, 2009. [Online accessed 02.05.2020].

- [61] Allan Seabridge Ian Moir. *Aircraft Systems: Mechanical, Electrical, and Avionics Subsystems Integration*. Wiley, 2001.
- [62] More electric aircraft: How does electricity work on a plane? https://www.safran-electrical-power.com/media/20151109_more-electric-aircraft-how-does-electricity-work-plane 2020. [Online accessed 25.04.2020].
- [63] Hugh Morris. How many planes are there in the world right now? <https://www.telegraph.co.uk/travel/travel-truths/how-many-planes-are-there-in-the-world/>, 2020. [Online accessed 27.04.2020].
- [64] Xiuxian Xia. Dynamic power distribution managementfor all electric aircraft. Master's thesis, CRANFIELD UNIVERSITY, SCHOOL OF ENGINEERING, 2011.
- [65] Ryan Morrison. Nasa reveals the first images of its all-electric x-57 maxwell plane that will be 500 per cent more efficient than conventional aircraft while producing zero emissions and less noise pollution. <https://www.dailymail.co.uk/sciencetech/article-8160459/NASA-reveals-images-electric-X-57-Maxwell-plane.html>, 2020. [On-line accessed 29.04.2020].
- [66] Accel: entering the era of zero-emissions aviation. <https://www.rolls-royce.com/innovation/key-demonstrators/accel.aspx#powertrain> 2020. [Online accessed 27.04.2020].
- [67] Michael Gubisch. Rolls-royce aims to break speed record with electric single-seater. <https://www.flightglobal.com/engines/rolls-royce-aims-to-break-speed-record-with-electric-single-seater/130880.article>, 2019. [Online accessed 27.04.2020].
- [68] Prachi Patel. The battery design smarts behind rolls royce's ultrafast electric airplane. <https://spectrum.ieee.org/energywise/energy/batteries-storage/the-battery-innovations-behind-rolls-royces-ultrafast-electric-airplane>, 2020. [Online accessed 29.04.2020].
- [69] Sebastian Schaal. Ampaire: Erstflug des größten hybrid-flugzeugs der welt. <https://www.electrive.net/2019/06/07/ampaire-erstflug-des-groessten-hybrid-flugzeugs-der-welt/>, 2019. [Online accessed 29.04.2020].
- [70] Barry Schiff. Ampaire 337 'parallel hybrid' unveiled. <https://www.aopa.org/news-and-media/all-news/2019/june/10/ampaire-337-parallel-hybrid-unveiled>, 2019. [Online accessed 29.04.2020].
- [71] uicontrol example. <https://wiki.octave.org/Uicontrols>, 2020. [Online accessed 20.06.2020].
- [72] uicontrol matlab documentation. <https://www.mathworks.com/help/matlab/ref/matlab.ui.control.uicontrol-properties.html> 2020. [Online accessed 20.06.2020].

- [73] Matlab indexation documentation. <https://www.mathworks.com/company/newsletters/articles/matrix-indexing-in-matlab.html>, 2020. [Online accessed 27.06.2020].
- [74] Benjamin Brelje and Joaquim Martins. Electric, hybrid, and turboelectric fixed-wing aircraft: A review of concepts, models, and design approaches. *Progress in Aerospace Sciences*, 104:1–19, 01 2019.
- [75] M. Voskuijl, Joris Bogaert, and Arvind Gangoli Rao. Analysis and design of hybrid electric regional turboprop aircraft. *CEAS Aeronautical Journal*, 9, 10 2017.
- [76] Reynard de Vries, Maurice Hoogreef, and Roelof Vos. Range equation for hybrid-electric aircraft with constant power split. *Journal of Aircraft*, pages 1–6, 04 2020.
- [77] Dornier 228 advanced commuter data sheet. <https://ruag.picturepark.com/Go/mqWBr0aEV/9760/1>, 2020. [Online accessed 23.06.2020].
- [78] Gas turbine efficiency. <https://www.wartsila.com/energy/learn-more/technical-comparisons/gas-turbine-for-power-generation-introduction>, 2020. [Online accessed 29.06.2020].
- [79] Kerosene co2 emissions 1. https://www.engineeringtoolbox.com/co2-emission-fuels-d_1085.html, 2020. [Online accessed 23.06.2020].
- [80] Kerosene co2 emissions 2. https://www.volker-quaschning.de/datserv/C02-spez/index_e.php, 2020. [Online accessed 23.06.2020].
- [81] Energy costs germany 2020. <https://www.statista.com/statistics/418078/electricity-prices-for-households-in-germany/>, 2020. [Online accessed 24.06.2020].
- [82] Day price kerosene. <https://www.indexmundi.com/de/rohstoffpreise/?ware=kerosin>, 2020. [Online accessed 24.06.2020].
- [83] Lift coefficient examples. <http://www.ae.utexas.edu/~varghesep/class/aircraft/Suggestions.pdf>, 2020. [Online accessed 24.06.2020].
- [84] Drag coefficient examples. <http://www.aerospaceweb.org/question/aerodynamics/q0184.shtml>, 2020. [Online accessed 24.06.2020].
- [85] Dornier 228 engine data sheet. <https://aerospace.honeywell.com/content/dam/aero/en-us/documents/learn/products/engines/brochures/N61-1491-000-000-TPE331-10TurbopropEngine-bro.pdf?download=true>, 2020. [Online accessed 24.07.2020].
- [86] Dornier 228 hourly fuel burn. https://hal-india.co.in/Product_Details.aspx?Mkey=54&1Key=&CKey=23, 2020. [Online accessed 26.07.2020].
- [87] Dornier 228 hourly fuel burn 2. <https://www.flightglobal.com/flight-test-ruags-dornier-228ng-put-to-the-test/106796.article>, 2020. [Online accessed 26.07.2020].
- [88] Thomas Gleason Paul Fahlstrom. *Introduction to UAV Systems*. 2012. [Online accessed 17.06.2020].

- [89] Mtr390 specific fuel consumption. https://www.mtu.de/fileadmin/DE/7_News_Media/2_Media/Broschueren/Engines/MTR390.pdf, 2020. [Online accessed 24.06.2020].
- [90] Michael Herrmann and Karl Heinz Pfestorf. *Öfen und Kamine : Raumheizungen fachgerecht planen und bauen, Bauwesen, Praxis*. Beuth;, Berlin, 2011.